arXiv:1304.2434v2 [physics.atom-ph] 26 Apr 2013

Antihydrogen ($\overline{\mathrm{H}}$) and muonic antihydrogen ($\overline{\mathrm{H}}_\mu$) formation in low energy three-charge-particle collisions

Renat A. Sultanov[a] and D. Guster[b]
Department of Information Systems & BCRL at St. Cloud State University,
Integrated Science and Engineering Laboratory Facility, St. Cloud, MN 56301-4498

(Dated: April 29, 2013)

Abstract

A few-body formalism is applied for computation of two different three-charge-particle systems. The first system is a collision of a slow antiproton, $\overline{\mathrm{p}}$, with a positronium atom: Ps= (e^+e^-) − a bound state of an electron and a positron. The second problem is a collision of $\overline{\mathrm{p}}$ with a muonic muonium atom, i.e. true muonium − a bound state of two muons one positive and one negative: $\mathrm{Ps}_\mu = (\mu^+\mu^-)$. The total cross section of the following two reactions: $\overline{\mathrm{p}} + (e^+e^-) \to \overline{\mathrm{H}} + e^-$ and $\overline{\mathrm{p}}+(\mu^+\mu^-) \to \overline{\mathrm{H}}_\mu+\mu^-$, where $\overline{\mathrm{H}} = (\overline{\mathrm{p}}e^+)$ is antihydrogen and $\overline{\mathrm{H}}_\mu = (\overline{\mathrm{p}}\mu^+)$ is a muonic antihydrogen atom, i.e. a bound state of $\overline{\mathrm{p}}$ and μ^+, are computed in the framework of a set of coupled two-component Faddeev-Hahn-type (FH-type) equations. Unlike the original Faddeev approach the FH-type equations are formulated in terms of only two but relevant components: Ψ_1 and Ψ_2, of the system's three-body wave function Ψ, where $\Psi = \Psi_1 + \Psi_2$. In order to solve the FH-type equations Ψ_1 is expanded in terms of the input channel target eigenfunctions, i.e. in this work in terms of, for example, the $(\mu^+\mu^-)$ atom eigenfunctions. At the same time Ψ_2 is expanded in terms of the output channel two-body wave functions, that is in terms of $\overline{\mathrm{H}}_\mu$ atom eigenfunctions. Additionally, a convenient total angular momentum projection is performed. This procedure leads to an infinite set of one-dimensional coupled integral-differential equations for unknown expansion functions. Since the two-body targets are treated equally and the accurate asymptotes of Ψ_1 and Ψ_2 are provided, the solution of the FH-type equations avoids the over-completeness problem. Results for better known low-energy μ^- transfer reactions from one hydrogen isotope to another hydrogen isotope in the cycle of muon catalyzed fusion (μCF) are also computed and presented.

PACS numbers: 36.10.Dr

---

[a] rasultanov@stcloudstate.edu (r.sultanov2@yahoo.com)
[b] dcguster@stcloudstate.edu

I. INTRODUCTION

To date, non-relativistic quantum-mechanical Coulomb few-body problems have a long research history. In fact, the first works dealing with quantum few-charged particle systems appeared during the early stages of quantum-mechanics [1]. This is because these types of problems pose significant fundamental theoretical and practical importance in nuclear and atomic-molecular physics. The few-body Coulomb problem is of considerable importance in the cycle of μCF (cold fusion) [2], in cases where a muonic few-body system experiences a strong interplay between Coulomb and nuclear forces involving heavy nuclei, for instance, the $(\mathrm{dt}\mu)^+$ molecular ion. Further, it would be worth mentioning that there are modern antimatter physics problems, that involve few-body systems, such as antihydrogen [3–8]/protonium [9–13] formation reactions, low energy $\overline{\mathrm{p}}+\mathrm{H}_2^+$ collisions [14], $\overline{\mathrm{H}}+\mathrm{H}_2$ quenching [15, 16], $\overline{\mathrm{H}}+\mathrm{H}$ annihilation reactions [17], and $\overline{\mathrm{p}}+{}^{4(3)}\mathrm{He}$ antiprotonic helium atom (atomcule) formation [18, 19] just to name a few. It follows from the charge conjugation, parity, and time reversal (CPT) symmetry of quantum electrodynamics that a charged particle and its antiparticle should have equal/opposite charges, equal masses, lifetimes, and gyromagnetic ratios. Moreover, the CPT symmetry predicts that hydrogen and antihydrogen atoms should have identical spectra. New experiments are in progress to test these fundamental laws and theories of physics involving antiparticles as well as antimatter in general. Therefore, future experimentalists plan to test whether H and $\overline{\mathrm{H}}$ have such properties. In such experiments, it would be important to have a certain quantity of $\overline{\mathrm{H}}$ atoms at low kinetic energies, ideally at the rest: $T \sim 0$ K [20, 21]. Using this perspective we develop a quantum-mechanical approach which would be reliable at low and very low collision energies, i.e. when the quantum-mechanical few-body dynamics of three Coulomb particles becomes important. The method is formulated for arbitrary masses of the particles, that is when the dynamics of lighter and heavier particles are not separated from each other.

The author of the book [22] pointed out that the muonic antihydrogen atom, $\overline{\mathrm{H}}_\mu$, could be even a better choice to check the CPT law than the usual antihydrogen atom. This is because the size of this atom is ~ 207 times smaller than the size of a normal $\overline{\mathrm{H}}$ atom. Therefore, as mentioned in [22]: the short range CPT violating interaction with an extremely heavy boson can be easily detected within the system. This idea appears be extremely interesting, and therefore it would be useful to compute the formation cross sections and rates of $\overline{\mathrm{H}}_\mu$ at low energy collisions, for example, from ∼1 eV down to $\sim 10^{-5}$ eV. Thus, in this work we consider the following three-body reactions of antihydrogen $\overline{\mathrm{H}}$ and muonic antihydrogen $\overline{\mathrm{H}}_\mu$ formation:

$$\overline{\mathrm{p}} + (e^+e^-)_{1s} \to \overline{\mathrm{H}} + e^-, \tag{1}$$

$$\overline{\mathrm{p}} + (\mu^+\mu^-)_{1s} \to \overline{\mathrm{H}}_\mu + \mu^-. \tag{2}$$

At such low energies the quantum-mechanical Coulomb few-body dynamics become important, especially in the case of heavy charge transfer, i.e. μ^+. Also, it would be quite appropriate to mention that exotic atomic and antiatomic systems like a true muonium atom, $(\mu^+\mu^-)$, or a simple muonic hydrogen atom, H_μ=$(\mathrm{p}^+\mu^-)$, are always of great interest in nuclear, atomic and few-body physics [23–25]. For instance, recently the authors of works [26, 27] have considered an interesting problem: the production of $(\mu^+\mu^-)$. This is the smallest pure QED atom with the Bohr radius only ∼512 fm. So far $(\mu^+\mu^-)$ has never been observed. Next, in the recent works [28, 29] the proton-radius puzzle [30] was considered from few-body and muonic physics perspectives. Another three-charge-particle reaction of $\overline{\mathrm{H}}_\mu$ formation was considered in the works [22, 25] too:

$$\overline{\mathrm{p}} + \mathrm{Mu} \to \overline{\mathrm{H}}_\mu + e^-. \tag{3}$$

Here, Mu is the muonium atom, i.e. a bound state of a positive muon μ^+ and an electron: Mu=(μ^+e^-). This is a very interesting and complex example of a heavy charge transfer reaction [25, 31].

In nuclear physics, involving applications related to three-body systems the few-body Faddeev and Alt-Grassberger-Sandhas (AGS) equations [32–35] are frequently employed. These equations are equal to the Schrődinger equation, but formulated for the three-body wave function components and therefore have the correct physical asymptotes. However, in the case of three-charged particle systems the kernels of the original integral Faddeev equations in momentum space lose their compactness due to Coulomb long-range interactions [33]. This limitation has become the most serious obstacle in the practical application of the original Faddeev equation to few-body systems with pure Coulomb interactions. Therefore, on one hand the Faddeev and AGS equations are the most rigorous attempt to provide a basis for detailed few-body numerical computations, but on the other hand they have not been used much to date because they have been regarded as too complex to solve when used in Coulomb scattering problems. This limitation has led to various alternative methods.

Among the most popular is a well known method based on the Born-Oppenheimer adiabatic model [36] and improved adiabatic approximation [37]. The approach has been applied to many systems in atomic and μ-atomic physics for over many years. Very accurate variational calculations have been applied to selected three-body Coulomb systems in muon catalyzed fusion cycle [38], and in $\overline{\mathrm{H}}$ formation reactions, see for instance [3]. Here it would also be useful to mention important Coulomb few-body calculations based on the adiabatic hyper-spherical method [6, 39], coordinate-space Faddeev equation approach in three dimensions [40] and within a hyper-spherical function expansion formalism [41]. There are also newer developments in the field we would also like to cite [42–44].

In the current work however we apply a different *few-body* approach based on a set of coupled two-component FH-type equation formalism [45–47]. The next section represents the notation pertinent to the three-charged-particle system (123) shown in Fig. 1, the original equations, boundary conditions, detailed derivation of the set of coupled one-dimensional integral-differential equations suitable for a numerical computation and the numerical computational approach developed in this work. Sec. III includes new results, conclusions, and Sec. IV includes Appendix. The atomic units, i.e. $e = \hbar = m_e = 1$, are used in the case of the e^+ transfer reaction, and the muonic units, i.e. $e = \hbar = m_\mu = 1$, are used in the case of the μ^+/μ^- transfer reactions, where $m_\mu = 206.769\ m_e$ is the mass of the muon.

II. FEW-BODY TREATMENT

In the case of three charged particles (123), two positive and one negative, only two asymptotic configurations are possible below the breakup threshold. This situation is shown in Fig. 2, for instance, for the $(\overline{\mathrm{p}}\ \mu^-\mu^+)$ system. It suggests to write down a set of two coupled equations for Faddeev-type components of the system's wave function [45]. These equations are commonly called Faddeev-Hahn-type (FH-type) equations [46]. In this work we shall consider a method based on an integral-differential equation approach [47] applied to Coulomb three-body systems. To solve these equations, a modified close coupling method is applied. This procedure leads to an expansion of the three-body system wave function components into eigenfunctions of the subsystem Hamiltonians, providing an infinite set of one-dimensional integral-differential equations [47]. Within this formalism the asymptotic of the full three-body wave function contains two parts corresponding to two open channels.

In this work we consider different Coulomb three-body systems with arbitrary masses, i.e. the masses of the charged particles are taken as they are. We do not apply any type of adiabatic approximations, when the dynamics of heavy and light parts of the system are separated.Therefore, this dynamical method works for both a light charge, e^+, transfer reaction at ultra-low energies and for heavy charge transfer, μ^+, as well.

A. FH-type equation approach

Let us define the system of units to be $e = \hbar = m_3 = 1$ and denote antiproton $\overline{\mathrm{p}}$ by 1, a negative muon μ^- by 2, and a positive muon μ^+ by 3. Before the three-body breakup threshold two cluster asymptotic configurations are possible in the three-body system, i.e. (23)−1 and (13)−2 being determined by their own Jacobi coordinates $\{\vec{r}_{j3}, \vec{\rho}_k\}$ as shown in Figs. 1, 2:

$$\vec{r}_{j3} = \vec{r}_3 - \vec{r}_j, \tag{4}$$

$$\vec{\rho}_k = (\vec{r}_3 + m_j\vec{r}_j)/(1 + m_j) - \vec{r}_k, \quad (j \neq k = 1, 2). \tag{5}$$

Here $\vec{r}_\xi$, m_ξ are the coordinates and the masses of the particles $\xi = 1, 2, 3$ respectively. This suggests a Faddeev formulation which uses only two components. A general procedure to derive such formulations is described in work [45]. In this approach the three-body wave function is represented as follows:

$$|\Psi\rangle = \Psi_1(\vec{r}_{23}, \vec{\rho}_1) + \Psi_2(\vec{r}_{13}, \vec{\rho}_2), \tag{6}$$

where each Faddeev-type component is determined by its own Jacobi coordinates. Moreover, $\Psi_1(\vec{r}_{23}, \vec{\rho}_1)$ is quadratically integrable over the variable $\vec{r}_{23}$, and $\Psi_2(\vec{r}_{13}, \vec{\rho}_2)$ over the variable $\vec{r}_{13}$. To define $|\Psi_l\rangle$, $(l = 1, 2)$ a set of two coupled Faddeev-Hahn-type equations can be written:

$$\Big(E - \hat{H}_0 - V_{23}(\vec{r}_{23})\Big)\Psi_1(\vec{r}_{23}, \vec{\rho}_1) = \Big(V_{23}(\vec{r}_{23}) + V_{12}(\vec{r}_{12})\Big)\Psi_2(\vec{r}_{13}, \vec{\rho}_2), \tag{7}$$

$$\Big(E - \hat{H}_0 - V_{13}(\vec{r}_{13})\Big)\Psi_2(\vec{r}_{13}, \vec{\rho}_2) = \Big(V_{13}(\vec{r}_{13}) + V_{12}(\vec{r}_{12})\Big)\Psi_1(\vec{r}_{23}, \vec{\rho}_1). \tag{8}$$

Here, $\hat{H}_0$ is the kinetic energy operator of the three-particle system, $V_{ij}(r_{ij})$ are paired interaction potentials $(i \neq j = 1, 2, 3)$, E is the total energy. The constructed equations satisfy the Schrődinger equation exactly. For the energies below the three-body break-up threshold they exhibit the same advantages as the Faddeev equations [33], because they are formulated for the wave function components with the correct physical asymptotes. To solve the equations a close-coupling method is applied, which leads to an expansion of the system's wave function components into eigenfunctions of the subsystem (target) Hamiltonians providing with a set of one-dimensional integral-differential equations after the partial-wave projection. A further advantage of the Faddeev-type method is the fact that the Faddeev-components are smoother functions of the coordinates than the total wave function. Also, the Faddeev decomposition avoids overcompleteness problems, because two-body subsystems are treated in an equivalent way, and the correct asymptotes are guaranteed. Next, based on Merkuriev [33, 34] the three-charge-particle scattering wave function and its all three components should have the following general asymptotic form:

$$\Psi_k(\vec{r}_{j3},\vec{\rho}_k) \underset{\rho_k\to+\infty}{\sim} e^{ik_1z}\varphi_1(\vec{r}_{j3})\delta_{k1} + \sum_n^{\infty} A_n^{el/ex}(\Omega_{\rho_k})\frac{e^{ik_n\rho_k}}{\rho_k}\varphi_n(\vec{r}_{j3}) + \sum_m^{\infty} A_m^{tr}(\Omega_{\rho_j})\frac{e^{ik'_m\rho_j}}{\rho_j}\varphi_m(\vec{r}_{k3}) + B(\Omega_5)\frac{e^{i(\sqrt{E}\rho+W^c(\rho,E)}}{\rho^{5/2}}. \tag{9}$$

Here, $e^{ik_1z}\varphi_1(\vec{r}_{j3})$ is the incident wave, $\varphi_n(\vec{r}_{j3})$ the $n-$th bound-state wave function of the pair $(j3)$, $k_n = (E-\varepsilon_n)^{1/2}$, ε_n is the binding energy of the $(j3)$, $A^{el/ex}(\Omega_{\rho_k})$, $A^{tr}(\Omega_{\rho_j})$ and $B(\Omega_5)$ are amplitudes of elastic/inelastic, transfer and breakup channels respectively, $\rho_6 = (\rho, \Omega_5)$ is the three-body hyperradius and $W^c(\rho, E)$ is the three-body Coulomb phase [34]. For lower energy collisions when $E < E_{thr}$, where E_{thr} is the three-body break-up threshold, the expression (9) becomes simpler, i.e. without the last term: $B(\Omega_5) = 0$.

Therefore, in the current work for low energy collisions each Faddeev type component corresponds to only one determined channel. For example, for the elastic and for the charge transfer channel we have:

$$\Psi_1(\vec{r}_{23},\vec{\rho}_1) \underset{\rho_1\to+\infty}{\sim} e^{ik_1z}\varphi_1(\vec{r}_{23}) + \sum_n^{\infty} A_n^{el/ex}(\Omega_{\rho_1})\frac{e^{ik_n\rho_1}}{\rho_1}\varphi_n(\vec{r}_{23}), \tag{10}$$

$$\Psi_2(\vec{r}_{13},\vec{\rho}_2) \underset{\rho_2\to+\infty}{\sim} \sum_m^{\infty} A_m^{tr}(\Omega_{\rho_2})\frac{e^{ik'_m\rho_2}}{\rho_2}\varphi_m(\vec{r}_{13}). \tag{11}$$

It is easy to see that the asymptotic behavior of the total wave function (6) becomes similar to equation (9).

In addition, we would like to point out, that the few-body FH-type equation approach (7)-(8) is a quite flexible method. For example, let us briefly consider a muon transfer reaction in the following low energy collision:

$$\mathrm{Li}^{3+} + (\mathrm{p}^+\mu^-)_{1\mathrm{s}} \rightarrow (\mathrm{Li}_\mu^{2+})_{1\mathrm{s}} + \mathrm{p}^+. \tag{12}$$

This reaction has a strong, pure Coulomb interaction in the output channel. This circumstance can be taken into account by adding a distortion potential into the FH equations (7)-(8), i.e. $U(\rho_2) = (Z_1 - 1)Z_2/\rho_2$, where Z_1 is the charge of Li^{3+} and $Z_2(=1)$ is the charge of the hydrogen isotope:

$$\Big(E - \hat{h}_{23}(\vec{r}_{23}) - \hat{T}_1(\vec{\rho}_1)\Big)\Psi_1(\vec{r}_{23}, \vec{\rho}_1) = \Big(V_{23}(\vec{r}_{23}) + V_{12}(\vec{r}_{12}) - \frac{(Z_1-1)Z_2}{\rho_2}\Big)\Psi_2^C(\vec{r}_{13}, \vec{\rho}_2), \tag{13}$$

$$\Big(E - \hat{h}_{13}(\vec{r}_{13}) - \hat{T}_2(\vec{\rho}_2) - \frac{(Z_1-1)Z_2}{\rho_2}\Big)\Psi_2^C(\vec{r}_{13}, \vec{\rho}_2) = \Big(V_{13}(\vec{r}_{13}) + V_{12}(\vec{r}_{12})\Big)\Psi_1(\vec{r}_{23}, \vec{\rho}_1). \tag{14}$$

The two coupled equations satisfy the Schrődinger equation exactly, i.e. when the Eqs. (13)-(14) are added to each other the two distortion potential terms vanish. Also, in these equations we identify the target hamiltonians $\hat{h}_{23}(\vec{r}_{23})$ and $\hat{h}_{13}(\vec{r}_{13})$, as well as the kinetic energy operators, i.e. $\hat{T}_1(\vec{\rho}_1)$ and $\hat{T}_2(\vec{\rho}_2)$. One can see, that by converting the differential Eq. (14) into an integral equation we can obtain a Coulomb Green function over the Jacobi coordinate ρ_2 in the output channel. The Green function provides the physically correct Coulomb asymptotic for the component $|\Psi_2^C\rangle$. The component $|\Psi_1\rangle$ carries the asymptotic behavior for the elastic and inelastic channels and the component $|\Psi_2^C\rangle$ carries the Coulomb asymptotic behavior in the transfer channel, that is:

$$\Psi_1(\vec{r}_{23}, \vec{\rho}_1) \underset{\rho_1 \to +\infty}{\sim} e^{ik_1^{(1)}z}\varphi_1(\vec{r}_{23}) \; + \; \sum_n A_n^{\mathrm{el/in}}(\Omega_{\rho_1})\frac{e^{ik_n^{(1)}\rho_1}}{\rho_1}\varphi_n(\vec{r}_{23}), \tag{15}$$

$$\Psi_2^C(\vec{r}_{13}, \vec{\rho}_2) \underset{\rho_2 \to +\infty}{\sim} \sum_{ml} A_{ml}^{\mathrm{tr}}(\Omega_{\rho_2})\frac{e^{i(k_m^{(2)}\rho_2 - \pi l/2 + \tau_l - \eta/2k_m^{(2)}\ln 2k_m^{(2)}\rho_2)}}{\rho_2}\varphi_m(\vec{r}_{13}). \tag{16}$$

Here, $e^{ik_1^{(1)}z}\varphi_1(\vec{r}_{23})$ is the incident wave, $\varphi_n(\vec{r}_{j3})$ the n-th excited bound-state wave function of the pair $(j3)$, $k_n^{(i)} = \sqrt{2M_i(E - E_n^{(j)})}$, with $M_i^{-1} = m_i^{-1} + (1+m_j)^{-1}$, where m_i represents the masses of the heavy particles p and Li^{3+}. Here $E_n^{(j)}$ is the binding energy of $(j3)$, $i \neq j = 1, 2$, $A^{\mathrm{el/in}}(\Omega_{\rho_1})$ and $A^{\mathrm{tr}}(\Omega_{\rho_2})$ are the scattering amplitudes in the elastic/inelastic and transfer channels. The Coulomb parameters in the second transfer channel are: $\tau_l = \arg\Gamma(l + 1 + i\eta/2k_m^{(2)})$ and $\eta = 2M_2(Z_1 - 1)/k_n^{(2)}$. One can see, that this approach simplifies the solution procedure and provides the correct asymptotic behavior for the solution below the three-body breakup threshold. Further, the few-body method has been successfully applied to different three-body muon transfer reactions [46].

B. Obtaining an infinite set of coupled integral-differential FH-type equations

Now, let us present the equations (7)-(8) in terms of the adopted notation

$$\Big(E + \frac{1}{2M_k}\triangle_{\vec{\rho}_k} + \frac{1}{2\mu_j}\triangle_{\vec{r}_{j3}} - V_{j3}\Big)\Psi_i(\vec{r}_{j3}, \vec{\rho}_k) = \Big(V_{j3} + V_{jk})\Psi_{i'}(\vec{r}_{k3}, \vec{\rho}_j\Big), \tag{17}$$

here $i \neq i' = 1, 2$, $M_k^{-1} = m_k^{-1} + (1+m_j)^{-1}$ and $\mu_j^{-1} = 1 + m_j^{-1}$. In order to separate angular variables, the wave function components Ψ_i are expanded over bipolar harmonics:

$$\{Y_\lambda(\hat{\rho}) \otimes Y_l(\hat{r})\}_{LM} = \sum_{\mu m} C^{LM}_{\lambda\mu l m} Y_{\lambda\mu}(\hat{\rho}) Y_{lm}(\hat{r}), \tag{18}$$

where $\hat{\rho}$ and $\hat{r}$ are angular coordinates of vectors $\vec{\rho}$ and $\vec{r}$; $C^{LM}_{\lambda\mu l m}$ are Clebsh-Gordon coefficients; Y_{lm} are spherical functions [48]. The configuration triangle of the particles (123) is presented on the Fig. 1 together with the Jacobi coordinates $\{\vec{r}_{23}, \vec{\rho}_1\}$ and $\{\vec{r}_{13}, \vec{\rho}_2\}$ and angles between them. The centre-off-mass of the whole three-body system is designated as O. The centre-off-masses of the two-body subsystems (23) and (13) are O_1 and O_2 respectively. Substituting the following expansion:

$$\Psi_i(\vec{r}_{j3}, \vec{\rho}_k) = \sum_{LM\lambda l} \Phi^i_{LM\lambda l}(\rho_k, r_{j3}) \{Y_\lambda(\hat{\rho}_k) \otimes Y_l(\hat{r}_{j3})\}_{LM} \tag{19}$$

into (17), multiplying this by the appropriate biharmonic functions and integrating over the corresponding angular coordinates of the vectors $\vec{r}_{j3}$ and $\vec{\rho}_k$, we obtain a set of equations which for the case of the central potentials has the form:

$$\Big(E + \frac{1}{2M_k\rho_k^2}\Big\{\frac{\partial}{\partial\rho_k}(\rho_k^2\frac{\partial}{\partial\rho_k}) - \lambda(\lambda+1)\Big\} + \frac{1}{2\mu_j r_{j3}^2}\Big\{\frac{\partial}{\partial r_{j3}}(r_{j3}^2\frac{\partial}{\partial r_{j3}}) - l(l+1)\Big\} - V_{j3}\Big)\Phi^i_{LM\lambda l}(\rho_k, r_{j3}) = \int d\hat{\rho}_k \int d\hat{r}_{j3} \sum_{\lambda' l'} W^{(ii')LM}_{\lambda l \lambda' l'} \Phi^{i'}_{LM\lambda' l'}(\rho_j, r_{k3}), \tag{20}$$

where the following notation has been introduced:

$$W^{(ii')LM}_{\lambda l \lambda' l'} = \{Y_\lambda(\hat{\rho}_k) \otimes Y_l(\hat{r}_{j3})\}^*_{LM} \Big(V_{j3} + V_{jk}\Big) \{Y_{\lambda'}(\hat{\rho}_j) \otimes Y_{l'}(\hat{r}_{k3})\}_{LM}. \tag{21}$$

To progress from (20) to one-dimensional equations, we apply a modified close coupling method, which consists of expanding each component of the wave function $\Psi_i(\vec{r}_{j3}, \vec{\rho}_k)$ over the Hamiltonian eigenfunctions of subsystems:

$$\hat{h}_{j3} = -\frac{1}{2\mu_j}\nabla^2_{\vec{r}_{j3}} + V_{j3}(\vec{r}_{j3}). \tag{22}$$

Thus, following expansions can be applied:

$$\Phi^i_{LM\lambda l}(\rho_k, r_{j3}) = \frac{1}{\rho_k}\sum_n f^{(i)LM}_{nl\lambda}(\rho_k) R^{(i)}_{nl}(r_{j3}), \tag{23}$$

where functions $R^i_{nl}(r_{j3})$ are defined by the following equation:

$$\Big(E^i_n + \frac{1}{2\mu_j r^2_{j3}}\Big\{\frac{\partial}{\partial r_{j3}}(r^2_{j3}\frac{\partial}{\partial r_{j3}}) - l(l+1)\Big\} - V_{j3}\Big) R^i_{nl}(r_{j3}) = 0. \tag{24}$$

Substituting Eq. (23) into (20), multiplying by the corresponding functions $R^i_{nl}(r_{j3})$ and integrating over $r^2_{j3}dr_{j3}$ yields a set of integral-differential equations for the unknown functions $f^i_{nl\lambda}(\rho_k)$:

$$\begin{aligned} &2M_k(E - E^i_n) f^i_\alpha(\rho_k) + \Big(\frac{\partial^2}{\partial\rho^2_k} - \frac{\lambda(\lambda+1)}{\rho^2_k}\Big) f^i_\alpha(\rho_k) = \\ &2M_k \sum_\alpha \int_0^\infty dr_{j3} r^2_{j3} \int d\hat{r}_{j3} \int d\hat{\rho}_k \frac{\rho_k}{\rho_j} Q^{ii'}_{\alpha\alpha'} f^{i'}_{\alpha'}(\rho_j), \end{aligned} \tag{25}$$

where

$$Q^{ii'}_{\alpha\alpha'} = R^i_{nl}(r_{j3}) W^{(ii')LM}_{\lambda l\lambda' l'} R^{i'}_{n'l'}(r_{k3}). \tag{26}$$

For brevity one can denote $\alpha \equiv nl\lambda$ ($\alpha' \equiv n'l'\lambda'$), and omit LM because all functions have to be the same. The functions $f^i_\alpha(\rho_k)$ depend on the scalar argument, but this set is still not one-dimensional, as formulas in different frames of the Jacobi coordinates:

$$\vec{\rho}_j = \vec{r}_{j3} - \beta_k \vec{r}_{k3}, \quad \vec{r}_{j3} = \frac{1}{\gamma}(\beta_k \vec{\rho}_k + \vec{\rho}_j), \quad \vec{r}_{jk} = \frac{1}{\gamma}(\sigma_j \vec{\rho}_j - \sigma_k \vec{\rho}_k), \tag{27}$$

with the following mass coefficients:

$$\beta_k = m_k/(1+m_k), \quad \sigma_k = 1 - \beta_k, \quad \gamma = 1 - \beta_k\beta_j \quad (j \neq k = 1, 2), \tag{28}$$

clearly demonstrate that the modulus of $\vec{\rho}_j$ depends on two vectors, over which integration on the right-hand sides is accomplished: $\vec{\rho}_j = \gamma\vec{r}_{j3} - \beta_k\vec{\rho}_k$. Therefore, to obtain one-dimensional integral-differential equations, corresponding to equations (25), we will proceed with the integration over variables $\{\vec{\rho}_j, \hat{\rho}_k\}$, rather than $\{\vec{r}_{j3}, \hat{\rho}_k\}$. The Jacobian of this transformation is γ^{-3}. Thus, we arrive at a set of one-dimensional integral-differential equations:

$$2M_k(E - E^i_n) f^i_\alpha(\rho_k) + \Big(\frac{\partial^2}{\partial\rho^2_k} - \frac{\lambda(\lambda+1)}{\rho^2_k}\Big) f^i_\alpha(\rho_k) = \frac{M_k}{\gamma^{-3}} \sum_{\alpha'} \int_0^\infty d\rho_j S^{ii'}_{\alpha\alpha'}(\rho_j, \rho_k) f^{i'}_{\alpha'}(\rho_j), \tag{29}$$

where functions $S^{ii'}_{\alpha\alpha'}(\rho_j, \rho_k)$ are defined as follows:

$$\begin{aligned} S^{ii'}_{\alpha\alpha'}(\rho_j, \rho_k) = 2\rho_j\rho_k \int d\hat{\rho}_j \int d\hat{\rho}_k R^i_{nl}(r_{j3}) \left\{Y_\lambda(\hat{\rho}_k) \otimes Y_l(\hat{r}_{j3})\right\}^*_{LM} \Big(V_{j3} + V_{jk}\Big) \\ \left\{Y_{\lambda'}(\hat{\rho}_j) \otimes Y_{l'}(\hat{r}_{k3})\right\}_{LM} R^{i'}_{n'l'}(r_{k3}) \;. \end{aligned} \tag{30}$$

One can show (see Appendix, Sect. IV) that fourfold multiple integration in equations (30) leads to a one-dimensional integral and the expression (30) could be determined for any orbital momentum value L:

$$\begin{aligned} S^{ii'}_{\alpha\alpha'}(\rho_j,\rho_k) = \frac{4\pi}{2L+1}[(2\lambda+1)(2\lambda'+1)]^{\frac{1}{2}}\rho_j\rho_k \int_0^\pi d\omega \sin\omega R^i_{nl}(r_{j3})\Big(V_{j3}(r_{j3}) + {} \\ V_{jk}(r_{jk})\Big) R^{i'}_{n'l'}(r_{k3}) \sum_{mm'} D^L_{mm'}(0,\omega,0) C^{Lm}_{\lambda 0 lm} C^{Lm'}_{\lambda' 0 l'm'} Y_{lm}(\nu_j,\pi) Y^*_{l'm'}(\nu_k,\pi)\ , \end{aligned} \tag{31}$$

where $D^L_{mm'}(0,\omega,0)$ are Wigner functions, ω is the angle between $\vec{\rho}_j$ and $\vec{\rho}_k$, ν_j is the angle between $\vec{r}_{k3}$ and $\vec{\rho}_j$, ν_k is the angle between $\vec{r}_{j3}$ and $\vec{\rho}_k$ (see the Fig. 1). Finally, we obtain an infinite set of coupled integral-differential equations for the unknown functions $f^1_\alpha(\rho_1)$ and $f^2_{\alpha'}(\rho_2)$ [47]:

$$\begin{aligned} \Big((k^i_n)^2 + \frac{\partial^2}{\partial\rho_i^2} - \frac{\lambda(\lambda+1)}{\rho_i^2}\Big) f^i_\alpha(\rho_i) = g \sum_{\alpha'} \sqrt{\frac{(2\lambda+1)(2\lambda'+1)}{(2L+1)}} \int_0^\infty d\rho_{i'} f^{i'}_{\alpha'}(\rho_{i'}) \\ \int_0^\pi d\omega \sin\omega R^i_{nl}(r_{i'3}) \Big(V_{i'3}(r_{i'3}) + V_{ii'}(r_{ii'})\Big) R^{i'}_{n'l'}(r_{i3}) \rho_{i'}\rho_i \\ \sum_{mm'} D^L_{mm'}(0,\omega,0) C^{Lm}_{\lambda 0 lm} C^{Lm'}_{\lambda' 0 l'm'} Y_{lm}(\nu_i,\pi) Y^*_{l'm'}(\nu_{i'},\pi). \end{aligned} \tag{32}$$

For the sake of simplicity $\alpha \equiv (nl\lambda)$ are quantum numbers of a three-body state and L is the total angular momentum of the three-body system, $g = 4\pi M_i/\gamma^3$, $k^i_n = \sqrt{2M_i(E - E^{i'}_n)}$, where $E^{i'}_n$ is the binding energy of the subsystem $(i'3)$, $M_1 = m_1(m_2+m_3)/(m_1+m_2+m_3)$ and $M_2 = m_2(m_1+m_3)/(m_1+m_2+m_3)$ are the reduced masses, $\gamma = 1 - m_i m_{i'}/((m_i+1)(m_{i'}+1))$, $D^L_{mm'}(0,\omega,0)$ the Wigner functions, $C^{Lm}_{\lambda 0 lm}$ the Clebsh-Gordon coefficients, Y_{lm} are the spherical functions, ω is the angle between the Jacobi coordinates $\vec{\rho}_i$ and $\vec{\rho}_{i'}$, ν_i is the angle between $\vec{r}_{i'3}$ and $\vec{\rho}_i$, $\nu_{i'}$ is the angle between $\vec{r}_{i3}$ and $\vec{\rho}_{i'}$. One can show that: $\sin\nu_i = (\rho_k r_{kj})/\gamma \sin\omega$, and $\cos\nu_i = (\beta\rho_i + \rho_k\cos\omega)/(\gamma r_{kj})$.

C. Boundary conditions, cross sections and numerical implementation

To find a unique solution to Eqs. (32) appropriate boundary conditions depending on the specific physical situation need to be considered. First we impose:

$$f^{(i)}_{nl}(0) \sim 0. \tag{33}$$

Next, for the three-body charge-transfer problems we apply the well known **K**−matrix formalism. This method has already been applied for solution of three-body problems in the framework of the coordinate space Faddeev equations [41]. For the present scattering problem with $i + (j3)$ as the initial state, in the asymptotic region, it takes two solutions to Eq.(32) to satisfy the following boundary conditions:

$$\begin{cases} f_{1s}^{(i)}(\rho_i) \underset{\rho_1 \to +\infty}{\sim} \sin(k_1^{(i)}\rho_i) + K_{ii}\cos(k_1^{(i)}\rho_i) \\ f_{1s}^{(j)}(\rho_j) \underset{\rho_j \to +\infty}{\sim} \sqrt{v_i/v_j} K_{ij} \cos(k_1^{(j)}\rho_j) \ , \end{cases} \tag{34}$$

where K_{ij} are the appropriate coefficients, and v_i $(i = 1, 2)$ is a velocity in channel i. With the following change of variables in Eq. (32):

$$\mathsf{f}_{1s}^{(i)}(\rho_i) = f_{1s}^{(i)}(\rho_i) - \sin(k_1^{(i)}\rho_i), \tag{35}$$

(i=1, 2) we get two sets of inhomogeneous equations which are solved numerically. The coefficients K_{ij} can be obtained from a numerical solution of the FH-type equations. The cross sections are given by the following expression:

$$\sigma_{ij} = \frac{4\pi}{k_1^{(i)2}} \left| \frac{\mathbf{K}}{1 - i\mathbf{K}} \right|^2 = \frac{4\pi}{k_1^{(i)2}} \frac{\delta_{ij} D^2 + K_{ij}^2}{(D-1)^2 + (K_{11} + K_{22})^2}, \tag{36}$$

where $(i, j = 1, 2)$ refer to the two channels and $D = K_{11}K_{22} - K_{12}K_{21}$. Also, from the quantum-mechanical unitarity principle one can derive that the scattering matrix $\mathbf{K} = \begin{pmatrix} K_{11} & K_{12} \\ K_{21} & K_{22} \end{pmatrix}$ has the following important feature:

$$K_{12} = K_{21}. \tag{37}$$

In this work the relationship (37) is checked for all considered collision energies in both antihydrogen cases, i.e. in $\overline{\mathrm{p}} + (e^+e^-)$ and in $\overline{\mathrm{p}} + (\mu^+\mu^-)$, and in the case of the muon transfer reactions.

As stated in Sec.II A the solution of the Eqs. (7)-(8) involving both components $\Psi_{1(2)}$ required that we apply the expansions (19) and (23) over the angle and the distance variables respectively. However, to obtain a numerical solution for the set of coupled Eqs. (32) we only include the -s and -p waves in the expansion (19) and limit n up to 2 in the Eq. (23). As a result we arrive at a truncated set of six coupled integral-differential equations, since in $\Psi_{1(2)}$ only 1s, 2s and 2p target two-body atomic wave-functions are included. This method represents a modified version of the close coupling approximation with six expansion functions. The set of truncated integral-differential Eqs. (32) is solved by a discretization procedure, i.e. on the right side of the equations the integrals over ρ_1 and ρ_2 are replaced by sums using the trapezoidal rule [49] and the second order partial derivatives on the left side are discretized using a three-point rule [49]. By this means we obtain a set of linear equations for the unknown coefficients $f_\alpha^{(i)}(k)$ $(k = 1, N_p)$:

$$\left[\, k_n^{(1)2} + D_{ij}^2 - \frac{\lambda(\lambda+1)}{\rho_{1i}^2} \right] f_\alpha^{(1)}(i) \;-\; \frac{M_1}{\gamma^3} \sum_{\alpha'=1}^{N_s} \sum_{j=1}^{N_p} w_j S_{\alpha\alpha'}^{(12)}(\rho_{1i}, \rho_{2j}) f_{\alpha'}^{(2)}(j) = 0, \tag{38}$$

$$-\frac{M_2}{\gamma^3} \sum_{\alpha=1}^{N_s} \sum_{j=1}^{N_p} w_j S_{\alpha'\alpha}^{(21)}(\rho_{2i}, \rho_{1j}) f_\alpha^{(1)}(j) \;+\; \left[k_{n'}^{(2)2} + D_{ij}^2 - \frac{\lambda'(\lambda'+1)}{\rho_{2i}^2} \right] f_{\alpha'}^{(2)}(i) = B_{\alpha'}^{21}(i). \tag{39}$$

Here, coefficients w_j are weights of the integration points ρ_{1i} and ρ_{2i} $(i = 1, N_p)$, N_s is the number of quantum states which are taken into account in the expansion (23). Next, D_{ij}^2 is the three-point numerical approximation for the second order differential operator: $D_{ij}^2 f_\alpha(i) = (f_\alpha(i-1)\delta_{i-1,j} - 2f_\alpha(i)\delta_{i,j} + f_\alpha(i+1)\delta_{i+1,j})/\Delta$, where Δ is a step of the grid $\Delta = \rho_{i+1} - \rho_i$. The vector $B_{\alpha'}^{21}(i)$ is: $B_{\alpha'}^{(21)}(i) = M_2/\gamma^3 \sum_{j=1}^{N_p} w_j S_{\alpha' 1s0}^{(21)}(i,j) \sin(k_1 \rho_j)$, and in symbolic-operator notations the set of linear Eqs. (38)-(39) has the following form: $\sum_{\alpha'=1}^{2\times N_s} \sum_{j=1}^{N_p} \mathbf{A}_{\alpha\alpha'}(i,j) \vec{f}_{\alpha'}(j) = \vec{b}_\alpha(i)$. The discretized equations are subsequently solved by the Gauss elimination method [50]. As can be seen from Eqs. (38)-(39) the matrix $\mathbf{A}$ should have a so-called block-structure: there are four main blocks in the matrix: two of them related to the differential operators and other two to the integral operators. Each of these blocks should have sub-blocks depending on the quantum numbers $\alpha = nl\lambda$ and $\alpha' = n'l'\lambda'$. The second order differential operators produce three-diagonal sub-matrixes [47]. However, there is no need to keep the whole matrix $\mathbf{A}$ in computer's operating (fast) memory. The following optimization procedure shows that it would be possible to reduce the memory usage by at least four times. Indeed, the numerical equations (38)-(39) can be written in the following way: $D_1 f^1 - M_1 \gamma^{-3} S^{12} f^2 = 0$, and $-M_2 \gamma^{-3} S^{21} f^1 + D_2 f^2 = b$. Here, D_1, D_2, S^{12} and S^{21} are sub-matrixes of $\mathbf{A}$. Now one can determine that: $f^1 = (D_1)^{-1} M_1/\gamma^3 S^{12} f^2$, where $(D_1)^{-1}$ is reverse matrix of D_1. Thereby one can obtain a reduced set of linear equations which are used to perform the calculations: $[D_2 - M_1 M_2 \gamma^{-6} S^{21} (D_1)^{-1} S^{12}]\, f^2 = b$ [47].

To solve the coupled integral-differential equations (32) one needs to first compute the angular integrals Eqs. (31). They are independent of energy E. Therefore, one needs to compute them only once and then store them on a computer's hard drive (or solid state drive) to support future computation of other observables, i.e. the charge-transfer cross-sections at different collision energies. The sub-integral expressions in (31) have a very strong and complicated dependence on the Jacobi coordinates ρ_i and $\rho_{i'}$. To calculate $S^{(ii')}_{\alpha\alpha'}(\rho_i, \rho_{i'})$ at different values of ρ_i and $\rho_{i'}$ an adaptable algorithm has been applied together with the following mathematical substitution: $\cos\omega = (x^2 - \beta_i^2\rho_i^2 - \rho_{i'}^2)/(2\beta_i\rho_i\rho_{i'})$. The angle dependent part of the equation can be written as the following one-dimensional integral:

$$S^{(ii')}_{\alpha\alpha'}(\rho_i, \rho_{i'}) = \frac{4\pi}{\beta_i}\frac{[(2\lambda+1)(2\lambda'+1)]^{\frac{1}{2}}}{2L+1}\int_{|\beta_i\rho_i-\rho_{i'}|}^{\beta_i\rho_i+\rho_{i'}} dx R^{(i)}_{nl}(x)\left[-1+\frac{x}{r_{ii'}(x)}\right] R^{(i')}_{n'l'}(r_{i3}(x))$$
$$\sum_{mm'} D^L_{mm'}(0,\omega(x),0) C^{Lm}_{\lambda 0lm} C^{Lm'}_{\lambda'0l'm'} Y_{lm}(\nu_i(x),\pi) Y^*_{l'm'}(\nu_{i'}(x),\pi). \quad (40)$$

We used a special adaptive FORTRAN subroutine from the work [51] in order to carry out the angle integration in (40). This recursive computer program, QUADREC, is a better, modified version of the well known program QUANC8 [50]. QUADREC provides a much higher quality, stable and more precise integration than does QUANC8 [51]. Therefore, our results for the three-particle muon transfer reactions presented in Table I are slightly different from those of our older work [46] where we used the less effective adaptive quadrature code QUANC8 for numerical computation of the angle integrals (40). The difference between these two results ranges from ∼9% to ∼15%. The expression (40) differs from zero only in a narrow strip, i.e. when $\rho_i \approx \rho_{i'}$. This is because in the considered three-body systems the coefficient β_i is approximately equal to one. Figures 3 and 4 show the angle integral 2-dimensional functions (surfaces) (40) for the ($\overline{\mathrm{p}}$ $\mu^-\mu^+$) system considered herein. For example, this might involve a few selected atomic/muonic transitions such as: $S^{(12)}_{1s:1s'}(\rho_1, \rho_2)$ and $S^{(12)}_{1s:2s'}(\rho_1, \rho_2)$. Only the input channel $\overline{\mathrm{p}} + (\mu^-\mu^+)$ of the reaction (2) potential surfaces are included. It is seen, that these surfaces have significantly different geometrical shapes and numerical values. Therefore, in order to obtain numerically reliable converged results it is necessary to adequately distribute a very large number of discretization points (up to 2200) between 0 and ∼90 atomic/muonic units. More points are taken near the origin where the interaction potentials are large and a smaller number of points are needed at larger distances.

III. RESULTS AND CONCLUSIONS

In this section we report our computational results. Five different three-body Coulomb systems have been computed in the framework of a *unique* quantum-mechanical method, i.e. the FH-type equation formalism (7)-(8). The few-body approach has been presented in previous sections. In order to solve the coupled equations (7)-(8) we use two different and independent sets of target expansion functions (23). This is shown in Fig. 2 for the case of the $(\mu^+\mu^-)$ and $(\overline{\mathrm{p}}\mu^+)$ targets. Together with the specific structure of the two coupled FH-type equations in the operator form this method allows us to avoid the over-completeness problem and the two targets are treated equivalently. The main goal of this work is to carry out a reliable quantum-mechanical computation of the formation cross sections and corresponding rates of the $\overline{\mathrm{H}}$ and $\overline{\mathrm{H}}_\mu$ atoms at very low collision energies, i.e. reactions (1) and (2). However, as a test of the method and our FORTRAN code we carried out calculations of the three-body cross sections and rates of the μ^- transfer reactions from d to t: t + $(\mathrm{d}\mu^-) \to (\mathrm{t}\mu^-)$ + d, from p to t: t + $(\mathrm{p}\mu^-) \to (\mathrm{t}\mu^-)$ + p, and from p to d: d + $(\mathrm{p}\mu^-) \to (\mathrm{d}\mu^-)$ + p. Here, p, d and t are the hydrogen isotopes: proton p=$^1\mathrm{H}^+$, deuterium d=$^2\mathrm{H}^+$, and tritium t=$^3\mathrm{H}^+$. The coupled integral-differential Eqs. (32) have been solved numerically for the case of the total angular momentum $L = 0$ within the two-level 2×(1s), four-level 2×(1s+2s), and six-level 2×(1s+2s+2p) close coupling approximations in Eq. (23). The sign "2×" indicates that two different sets of expansion functions are applied. Next, the following boundary conditions (33), (34), and (35) have been used. To compute the charge transfer cross sections the expression (36) has been applied.

It would be useful to make a comment about the behaviour of $\sigma_{tr}(\varepsilon_{coll})$ at very low collision energies: $\varepsilon_{coll} \sim 0$. From our calculation we found that the muon transfer cross sections $\sigma_{tr} \to \infty$ as $\varepsilon_{coll} \to 0$. However, the muon transfer rates, λ_{tr}, are proportional to the product $\sigma_{tr} \times v_{c.m.}$ and this trends to a finite value as $v_{c.m.} \to 0$. Here $v_{c.m.} = \sqrt{2\varepsilon_{coll}/M_k}$ is a relative center-of-mass velocity between the particles in the input channel of the three-body reactions, and M_k is the reduced mass. To compute the muon transfer rate the following formula is used:

$$\lambda_{tr} = \sigma_{tr}(\varepsilon_{coll} \to 0) v_{c.m.} N_0, \tag{41}$$

where $N_0 = 4.25 \cdot 10^{22}\mathrm{c.m.}^3$ is the liquid hydrogen density.

The Coulomb few-body systems mentioned above are of a significant importance in the μCF cycle [2]. In the literature one can find the results of a variety of different calculations of these reactions. We compare our results with some of this data. Table I shows cross sections, σ_{tr}, and corresponding thermal rates, λ_{tr}, for all three muon transfer reactions at low collision energies together with some theoretical calculations from older papers [36–38, 43] and with some experimental data from works [52–58]. Our FH-type equation results shown in Table I have been computed within the 2×(1s+2s+2p) approximation in the expansion (23) for both Faddeev-type components.Therefore, it was actually used with up to six expansion functions. One can see that our σ_{tr} and λ_{tr} are in fairly good agreement with previous calculations and experimental data for *all three muonic systems* presented in Table I. The largest number of results can be found for the first listed reaction, i.e. d+(tμ^-), which is one of the most important three-particle reactions in the μCF cycle in cold liquid hydrogen. We obtained very good agreement with the experimental data and with some theoretical results, except in the case of work [37]. A very good agreement is also obtained for the other two reactions: for t+(pμ^-) and d+(pμ^-). These results show that the few-body method of the two coupled FH-type equation (7)-(8) works extremely well together with the close coupling expansion method (23). Only three therms in the expansion (23), i.e. 2×(1s+2s+2p) approximation, can provide such good agreement with the experiments for all three muonic transfer reactions. As we already mentioned the sign ”2×” means that the three term expansion is used within two different expansion functions sets. Figs. 5 and 6 show our cross sections for t+(pμ^-) and d+(pμ^-) collisions. Again, these results are obtained within the different close coupling expansion approximations: 2×1s, 2×(1s+ 2s), and 2×(1s+2s+2p). In the first case only two expansion functions are used, in the second case only four, and in the third case six expansion functions are used. One can see how significantly the 2p-state contributes to the total muon transfer cross section when decreasing the collision energy, especially this is seen in the case of d+(pμ^-). A comparison with the experimental data and other theoretical results in Table I for all three muonic transfer reactions demonstrates that the FH-type equations and 2×(1s+2s+2p) approximation are able to provide reliable results for three-body charge transfer reactions at low energies. It is also important to mention here, that the pure quantum-mechanical behaviour of the transfer cross section at low energies, specifically $\sigma_{tr}(\varepsilon_{coll} \sim 0) \sim 1/v_{c.m.}$, has been obtained in this calculation. This allowed us to compute the muon transfer rates (41), i.e. $\lambda_{tr}(T \to 0) \approx$const, and compare these results with the experiments.

Next, the three-body reaction of the atomic $\overline{\mathrm{H}}$ formation, i.e. reaction (1) is considered. We are primarily interested in low energy collisions. Because this is not a muonic system one needs to switch from muonic to atomic units. Also, in the computer program one needs to change the masses of the particles. Fig. 7 shows our results for the reaction (1) total cross section in the framework of different close-coupling approximations in the Eq. (23). One can see, that the contribution of the 2p-states in each target become larger while the collision energy becomes smaller. As in the muonic transfer reactions we found that the cross section of the $\overline{\mathrm{H}}$ formation $\sigma_{\overline{\mathrm{H}}} \to \infty$ as $\varepsilon_{coll} \to 0$, i.e. $\sigma_{\overline{\mathrm{H}}} v_{c.m.} \approx$const. This fact allows us to compute the low energy rate of the $\overline{\mathrm{H}}$ production. For example, one can follow the logic of work [3] and estimate the $\overline{\mathrm{H}}$ production rate by using the following formula: $R_{\overline{\mathrm{H}}} = \sigma_{\overline{\mathrm{H}}} N_{\overline{\mathrm{p}}} l I$. According to [3] $N_{\overline{\mathrm{p}}}$ is the density of slow antiprotons, I is the number of $\overline{\mathrm{p}}$ traversing the interaction region each second, and l is the linear dimension of the interaction region. In [3] the last parameter was taken as $l = 1$ cm. The product of lI has the unit of velocity, thus it should be possible to represent the rate $R_{\overline{\mathrm{H}}}$ as well as the expression (41), i.e.:

$$R_{\overline{\mathrm{H}}} = \sigma_{\overline{\mathrm{H}}}\ v_{c.m.} N_{\overline{\mathrm{p}}}, \tag{42}$$

where $v_{c.m.}$ is the c.m. velocity between $\overline{\mathrm{p}}$ and the positronium atom Ps. Our results for $\overline{\mathrm{H}}$ are shown in Table II together with the results for the $\overline{\mathrm{H}}_{\mu}$ formation reaction (2). At low energies $R_{\overline{\mathrm{H}}}$ starts taking a constant value as was the case in our previous calculation of the μ^- transfer reactions. It would be interesting to estimate the $N_{\overline{\mathrm{p}}}$ parameter. For example, if we accept the recent data from the Evaporative Cooling (EC) experiment at the Antiproton Decelerator (AD) at CERN [20]: n_{EC} ≈4000 very cold $\overline{\mathrm{p}}$ at $T_{EC} \approx 9$ K, we would need to place this quantity of antiprotons in a limited space with a volume $V_{\overline{\mathrm{p}}}^{EC}$. The temperature T_{EC} corresponds to the low energy collisions considered in this work: $\sim 10^{-4}$ eV. In order to obtain the rate $R_{\overline{\mathrm{H}}} \gtrsim 1$, one would need the following volume: $V_{\overline{\mathrm{p}}}^{EC} \approx 4000 \sigma_{\overline{\mathrm{H}}}\ v_{c.m.} = 4000 \times 6.68 \times 10^{-9} \approx 27 \times 10^{-6}$ cm^3, where the value for $\sigma_{\overline{\mathrm{H}}}\ v_{c.m.}$ is taken from Table II. If we suppose that the interaction region between $\overline{\mathrm{p}}$ and the Ps atoms has a cylindrical shape with the length $l_0 = 1$ cm [3], its radius r_0 should be: $r_0 \sim 8.6 \times 10^{-3}$ cm. As one can see r_0 has a very small value, although it seems to us that it still would be possible to adopt this value in some experiments. However, a different situation arises if we adopt the results of a newer experiment on Adiabatic Cooling (AC) of antiprotons [21]. The authors of this work obtained 3×10^6 cold antiprotons at temperature 3.5 K! In this case one would need the following volume: $V_{\overline{\mathrm{p}}}^{AC} \approx 3 \times 10^6 \sigma_{\overline{\mathrm{H}}}\ v_{c.m.} = 3 \times 10^6 \times 6.68 \times 10^{-9} \approx 20 \times 10^{-3}$ cm^3. It is easy to compute that in this case the radius is $r_0 \sim 0.1$ cm. Finally, Fig. 8 shows our results for the $\overline{\mathrm{H}}_{\mu}$ formation cross section. It is clear that in the process (2) the contribution of the 2p-states from each target is becoming even more significant while the collision energy becomes smaller. Additionally, for the process (2) we also compute the numerical value of the quantity: $\sigma_{\overline{\mathrm{H}}_\mu}(\varepsilon_{coll} \to 0)v_{c.m.} \approx$ const. Table II includes our data for this important parameter together with the $\overline{\mathrm{H}}_\mu$ formation total cross section. All these results are obtained in the framework of the 2×(1s+2s+2p) close coupling approximation. These data can be useful in future developments of low energy collision experiments with participation of cold antiprotons and true muonium atoms. Next, because of the complexity of the few-body method, in this work only the total orbital momentum $L = 0$ has been taken into account. It was adequate in the case of slow and ultraslow collisions discussed above. However, to take into account the important contribution of higher L's at higher collision energies it would be possible to use Takayanig's Modified Wave Number Approximation (MWNA) method [59]. In the recent work [60] the MWNA method has been successfully applied to a few-body charge transfer reaction. In conclusion, it is feasible to expect that the FH-type equation formalism (7)-(8) could also be an effective tool for computation of the quite intriguing three-body reaction (3). This is another process of the $\overline{\mathrm{H}}_\mu$ atom production with a heavy charge transfer from one center to another [25, 31]. It would be interesting to compare the reaction rates of both processes (2) and (3) [22]. An additional point to emphasize would be that in some sense the reaction (3) and the few-body protonium (Pn) formation reaction [9–13] show close similarities. Therefore, it would be good to try to apply the FH-type equation method to the Pn formation problem too. Also, it seems quite possible to expand in some way or another the FH-type few-body equation approach and the modified close-coupling expansion method, Eqs. (19) and (23), to very important but challenging low-energy four-particle rearrangement scattering collisions with the pure Coulomb interaction between the particles, such as $\overline{\mathrm{H}}+\mathrm{H}\to (\overline{\mathrm{p}}\mathrm{p}^+)_{\mathrm{nl}}+(\mathrm{e}^+\mathrm{e}^-)_{\mathrm{n'l'}}$ or, for example, $\overline{\mathrm{H}}_\mu+\mathrm{H}_\mu \to (\overline{\mathrm{p}}\mathrm{p}^+)_{\mathrm{nl}}+(\mu^+\mu^-)_{\mathrm{n'l'}}$.

IV. APPENDIX

The details of the derivation of the angular integrals $S^{ii'}_{\alpha\alpha'}(\rho_j, \rho_k)$ (31) are explained below in this section. The configuration triangle, $\triangle(123)$, is determined by the Jacobi vectors $(\vec{r}_{j3}, \vec{\rho}_k)$ and should be considered in an arbitrary coordinate system $OXYZ$. In this initial system the angle variables of the three-body Jacobi vectors $\{\vec{r}_{j3}, \vec{\rho}_k\}$ have the following values: $\hat{r}_{j3} = (\theta_j, \phi_j),\ \hat{\rho}_k = (\Theta_k, \Phi_k),\ j \neq k = 1, 2$. Let us adopt a new coordinate system $O'X'Y'Z'$ in which the axis $O'Z'$ is directed over the vector $\vec{\rho}_k$, $\triangle(123)$ belongs to the plain

$O'X'Z'$ and the vertex $k = 1$ of $\triangle(123)$ coincides with the origin O' of the new $OX'Y'Z'$. Fig. 9 shows the specific configuration of $\triangle(123)$ and the new adopted $O'X'Y'Z'$ system. One can see, that the new angle variables of the Jacobi vectors in the $O'X'Y'Z'$ system have now the following values: $\hat{r}'_{j3} = (\nu_k, \pi)$, $\hat{\rho}'_k = (0, 0)$, $\hat{r}'_{k3} = (\eta_k, \pi)$, $\hat{\rho}'_j = (\omega, \pi)$, here $k = 1$ and $j = 2$. The spatial rotational transformation from $OXYZ$ to $O'X'Y'Z'$ has been done with the use of the following Euler angles $(\Phi_k, \Theta_k, \varepsilon)$ [48]. Taking into account the transformation rule for the bipolar harmonics between new and old coordinate systems, one can write down the following relationships [48]:

$$\{Y_\lambda(\hat{\rho}_k) \otimes Y_l(\hat{r}_{j3})\}^*_{LM} = \sum_m (D^L_{Mm}(\Phi_k, \Theta_k, \varepsilon))^* \left\{Y_\lambda(\hat{\rho}'_k) \otimes Y_l(\hat{r}'_{j3})\right\}^*_{Lm} \tag{43}$$

$$\{Y_{\lambda'}(\hat{\rho}_j) \otimes Y_{l'}(\hat{r}_{k3})\}_{LM} = \sum_{m'} D^L_{Mm'}(\Phi_k, \Theta_k, \varepsilon) \left\{Y_{\lambda'}(\hat{\rho}'_j) \otimes Y_{l'}(\hat{r}'_{k3})\right\}_{Lm'} , \tag{44}$$

where $D^L_{Mm}(\Phi_k, \Theta_k, \varepsilon)$ are the Wigner functions [48]. The fourfold multiple angular integration $\int d\hat{\rho}_j \int d\hat{\rho}_k$ in Eq. (30) can be written in the new variables and be symbolically represented as $\int d\hat{\rho}_j \int d\hat{\rho}_k = \int_0^\pi d\omega \sin\omega \int_0^{2\pi} d\varepsilon \int_0^{2\pi} d\Phi_k \int_0^\pi \sin\Theta_k d\Theta_k$. Next, taking into account the normalizing condition for the Wigner functions [48]:

$$\int_0^{2\pi} d\varepsilon \int_0^{2\pi} d\Phi_k \int_0^\pi \sin\Theta_k d\Theta_k (D^L_{Mm}(\Phi_k, \Theta_k, \varepsilon))^* D^L_{Mm'}(\Phi_k, \Theta_k, \varepsilon)) = \frac{8\pi^2}{2L+1}\delta_{mm'} \tag{45}$$

one can obtain the following intermediate expression:

$$S^{ii'}_{\alpha\alpha'}(\rho_j, \rho_k) = 2\rho_j\rho_k \sum_m \frac{8\pi^2}{2L+1} \int_0^\pi d\omega \sin\omega R^i_{nl}(r_{j3}) \left\{Y_\lambda(0,0) \otimes Y_l(\hat{r}'_{j3})\right\}^*_{Lm}$$
$$(V_{j3} + V_{jk}) \left\{Y_{\lambda'}(\hat{\rho}'_j) \otimes Y_{l'}(\hat{r}'_{k3})\right\}_{Lm'} R^{i'}_{n'l'}(r_{k3}) \ . \tag{46}$$

Now, let us make the next transformation of $\triangle(123)$ in which the vertex $j = 2$ of $\triangle(123)$ coincides with the centre O' of the $O'X'Y'Z'$ and $O'XYZ$, however the axis $O'Z''$ is directed along $\vec{\rho}_j$ and $\triangle(123)$ belongs to the plain $O'X''Z''$. This transformation, which converts the coordinate frame $O'X'Y'Z'$ into $O'X''Y''Z''$ is characterized by the following Euler angles $(0, \omega, 0)$. Therefore the vectors $(\vec{r}_{k3}, \vec{\rho}_j)$ have the following new variables: $\hat{r}''_{k3} = (\nu_j, \pi)$, $\hat{\rho}''_j = (0, 0)$. As a result of this rotation one can write down the following relationship:

$$\left\{Y_{\lambda'}(\hat{\rho}'_j) \otimes Y_{l'}(\hat{r}'_{k3})\right\}_{Lm} = \sum_{m'} D^L_{Mm'}(0, \omega, 0) \left\{Y_{\lambda'}(\hat{\rho}''_j) \otimes Y_{l'}(\hat{r}''_{k3})\right\}_{Lm'} \tag{47}$$

and obtain the following result:

$$S^{ii'}_{\alpha\alpha'}(\rho_j, \rho_k) = 2\rho_j\rho_k \sum_{mm'} \frac{8\pi^2}{2L+1} \int d\omega \sin\omega R^i_{nl}(r_{j3}) \left\{Y_\lambda(0,0) \otimes Y_l(\hat{r}'_{j3})\right\}^*_{Lm} (V_{j3} + V_{jk})$$
$$D^L_{mm'}(0, \omega, 0) \left\{Y_{\lambda'}(0,0) \otimes Y_{l'}(\hat{r}''_{k3})\right\}_{Lm'} R^{i'}_{n'l'}(r_{k3}). \tag{48}$$

Now by taking into account that $Y_{lm}(0,0) = \delta_{m,0}\sqrt{(2l+1)/4\pi}$ [48], the bipolar harmonics in (48) are:

$$\{Y_\lambda(0,0) \otimes Y_l(\nu_k,\pi)\}^*_{Lm} = \sqrt{\frac{2\lambda+1}{4\pi}} C^{Lm}_{\lambda 0 lm} Y^*_{lm}(\nu_k,\pi), \tag{49}$$

$$\{Y_{\lambda'}(0,0) \otimes Y_{l'}(\nu_j,\pi)\}_{Lm'} = \sqrt{\frac{2\lambda'+1}{4\pi}} C^{Lm'}_{\lambda' 0 l' m'} Y_{l'm'}(\nu_j,\pi), \tag{50}$$

with the use of these relationships we finally get the convenient for numerical computations Eq. (31).

[1] M. Born and R. Oppenheimer, Ann. Phys., Liepzig, **84**, 457 (1927).

[2] K. Nagamine and L. Ponomarev, Nucl.Phys. A **721**, 863c (2003).

[3] J. W. Humberston, M. Charlton, F.M. Jacobsen, and B.I. Deutch, J. Phys. B: At. Mol. Opt. Phys. **20**, L25 (1987).

[4] M. Charlton, Phys. Lett. A **143**, 143 (1990).

[5] J. Mitroy and A.T. Stelbovics, J. Phys. B: At. Mol. Opt. Phys. **27**, L79 (1994).

[6] A. Igarashi, N. Toshima, and T. Shirai, J. Phys. B: At. Mol. Opt. Phys. **27**, L497 (1994).

[7] J. Mitroy and G. Ryzhikh, J. Phys. B: At. Mol. Opt. Phys. **30**, L371 (1997).

[8] N. Yamanaka and Y. Kino, Phys. Rev. A**65**, 062709 (2002); Nucl. Instr. Meth. Phys. Res. B**214**, 40 (2004).

[9] K. Sakimoto, Phys. Rev. A **65**, 012706 (2001).

[10] B.D. Esry and H.R. Sadeghpour, Phys. Rev. A **67**, 012704 (2003).

[11] S.Y. Ovchinnikov and J.H. Macek, Phys. Rev. A **71**, 052717 (2005).

[12] X.M. Tong, K. Hino, and N. Toshima, Phys. Rev. Lett. **97**, 243202 (2006)

[13] A. Igarashi and N. Toshima, Eur. Phys. J. D **46**, 425 (2008).

[14] K. Sakimoto, J. Phys. B: Atomic, Molecular and Optical Physics **37** 2255 (2004).

[15] M. R. Gregory and E. A. G. Armour, Nucl. Instrum. Methods Phys. Res. B **266**, 374 (2008).

[16] R.A. Sultanov, S.K. Adhikari, and D. Guster, Phys. Rev. A **81**, 022705 (2010).

[17] S. Jonsell, A. Saenz, P. Froelich, B. Zygelman, and A. Dalgarno, Phys. Rev. A **64**, 052712 (2001).

[18] T. Yamazaki, N. Morita, R.S. Hayano, E. Widmann, J. Eades, Phys. Rep. **366**, 183 (2002).

[19] R.S. Hayano, M. Hori, D. Horvath, Rep. Prog. Phys. **70**, 1995 (2007).

[20] G.B. Andresen et al., (ALPHA Collaboration), Phys. Rev. Lett. **105**, 013003 (2010).

[21] G. Gabrielse et al., (ATRAP Collaboration), Phys. Rev. Lett. **106**, 073002 (2011).

[22] K. Nagamine, *Introductory Muon Science* (Cambridge University Press, 2003); AIP Conf. Proc. **793**, 159 (2005).

[23] A. Ohsaki, T. Watanabe, K. Nakanishi, and K. Iguchi, Phys. Rev. A**32**, 2640 (1985).

[24] J. Cohen, J. Phys. B: At. Mol. Opt. Phys. **31**, L833 (1998).

[25] J. Cohen, Rep. Prog. Phys. **67**, 1769 (2004).

[26] S.J. Brodsky and R. F. Lebed, Phys. Rev. Lett. **102**, 213401 (2009).

[27] A. Banburski, and P. Schuster, Phys. Rev. D **86**, 093007 (2012).

[28] J.-P. Karr and L. Hilico, Phys. Rev. Lett. **109**, 103401 (2012).

[29] D. Tucker-Smith, I. Yavin, Phys. Rev. D **83** (10), 101702 (2011).

[30] R. Pohl et al., Nature **466**, 213 (2010).

[31] P. Kammel and K. Kubodera, Annu. Rev. Nucl. Part. Sci. **60**, 327 (2010)

[32] L.D. Faddeev, ZhETF (USSR) **39** 1459 (1960) [JETP (Sov. Phys.) **12**, 1014 (1961)].

[33] L.D. Faddeev and S.P. Merkuriev, *Quantum Scattering Theory for Several Particle Systems* (Kluwer Academic Publishers, Dordrecht, The Netherlands, 1993).

[34] S.P. Merkuriev, Ann. Phys. **130**, 395 (1980).

[35] E.O. Alt, P. Grassberger, and W. Sandhas, Nucl. Phys. B **2**, 167 (1967).

[36] A. Adamczak, C. Chiccoli, V. I. Korobov, V. S. Melezhik, P. Pasini, L. I. Ponomarev, and J. Wozniak, Phys. Lett. B **285**, 319 (1992).

[37] J.S. Cohen and M.C. Struensee, Physical Review A **43**, 3460 (1991).

[38] Y. Kino and M. Kamimura, Hyper. Inter. **82**, 45 (1993).

[39] A. Igarashi, N. Toshima, and T. Shirai, Phys. Rev. A **50**, 4951 (1994).

[40] A.A. Kvitsinsky and Chi-Yu Hu, Phys. Rev. A **47**, R3476 (1993).

[41] A.A. Kvitsinsky, J. Carbonell, C. Gignoux, Physical Review A **51**, 2997 (1995).

[42] E.A.G. Armour, J. -M. Richard, K. Varga, Physics Reports **413**, 1 (2005).

[43] A.V. Matveenko, E.O. Alt, and H. Fukuda, J. Phys. B: Atom., Mol. Opt. Phys. **42**, 165003 (2009).

[44] S. Jonsell, E.A.G. Armour, M. Plummer, Y. Liu, A.C. Todd, New J. Phys. **14**, 35013 (2012).

[45] Y. Hahn and K. Watson, Phys. Rev. A **5**, 1718 (1972).

[46] R.A. Sultanov and S.K. Adhikari, Phys. Rev. A, **61**, 022711 (2000); ibid. **62**, 022509 (2000).

[47] R.A. Sultanov and D. Guster, J. Comp. Phys. **192**, 231 (2003).

[48] D.A. Varshalovich, A.N. Moskalev, and V. K. Khersonskii, *Quantum Theory of Angular Momentum* (World Scientific Publish. Co., Singapore, 1988).

[49] M. Abramowitz and I. A. Stegun, *Handbook of Mathematical Functions: with Formulas, Graphs, and Mathematical Tables*, (Dover Publications, New York, 1965).

[50] G.E. Forsythe, M.A. Malcolm, and C.B. Moler, *Computer Methods in Mathematical Computations* (Prentice-Hall, Inc., Englewood Cliffs, New Jersey 1977).

[51] A.N. Berlizov and A.A. Zhmudsky, arXiv:physics/9905035v2.

[52] V. P. Dzhelepov, P. F. Ermolov, E. A. Kushnirenko, V. I. Moskalev, and S. S. Gershtein, Zh. Eksp. Theor. Fiz. **42**, 439 (1962) [Sov. Phys. JETP **15**, 306 (1962)].

[53] E. J. Bleser, E. W. Anderson, L. M. Lederman, S. L. Meyer, J. L. Rosen, J. E. Rothberg, and I-T. Wang, Phys. Rev. **132**, 2679 (1963).

[54] A. Bertin, M. Bruno, V. Vitale, A. Placci, and E. Zavattini, Lett. Nuovo Cimento **4**, 449 (1972).

[55] F. Mulhauser, J. L. Beveridge, G. M. Marshall, J. M. Bailey, G. A. Beer, P. E. Knowles, G. R. Mason, A. Olin, M. C. Fujiwara, T. M. Huber, R. Jacot-Guillarmod, P. Kammel, J. Zmeskal, S. K. Kim, A. R. Kunselman, V. E. Markushin, C. J. Martoff, and C. Petitjean, Phys. Rev. A **53**, 3069 (1996).

[56] V. M. Bystritsky, V. P. Dzhelepov, Z. V. Yershova, V. G. Zinov, V. K. Kapyshev, S. S. Mukhametgaleyeva, V. S. Nadezhdin, L. A. Rivkis, A. I. Rudenko, V. I. Satarov, N. V. Sergeyeva, L. N. Somov, V. A. Stolupin, and V. V. Filchenkov, Zh. Eksp.Teor. Fiz. **80**, 1700 (1980) [Sov. Phys. JETP **53**, 877 (1981)].

[57] S. E. Jones, A. N. Anderson, A. J. Caffrey, J. B. Walter, K. D. Watts, J. N. Bradbury, P. A. M. Gram, M. Leon, H. R. Maltrud, and M. A. Paciotti, Phys. Rev. Lett. **51**, 1757 (1983).

[58] W. H. Breunlich, M. Cargnelli, P. Kammel, J. Marton, N. Naegele, P. Pawlek, A. Scrinzi, J. Werner, J. Zmeskal, J. Bistirlich, K. M. Crowe, M. Justice, J. Kurck, C. Petitjean, R. H. Sherman, H. Bossy, H. Daniel, F. J. Hartmann, W. Neumann, and G. Schmidt, Phys. Rev. Lett. **58**, 329 (1987).

[59] K. Takayanagi, Adv. At. Mol. Phys. **1**, 149 (1965).

[60] R.A. Sultanov and D. Guster, Few-Body Systems (2013) Article in press, pp. 1-4 (DOI: 10.1007/s00601-013-0643-z).

TABLE I. Cross sections σ_{tr} and rates λ_{tr}, Eq. (41), for μ^- transfer reactions from a light hydrogen isotope to a heavier hydrogen isotope at low collision energies together with other theoretical results and experimental data. The result for unitarity ratio K_{21}/K_{12}, Eq. (37), are also presented for t+$(d\mu)_{1s}$.

Energy, eV	Method	t+$(d\mu)_{1s} \to (t\mu)_{1s}$+d			t+$(p\mu)_{1s} \to (t\mu)_{1s}$+p		d+$(p\mu)_{1s} \to (d\mu)_{1s}$+p	
		$\sigma_{tr}/10^{-20}$, cm^2	$\lambda_{tr}/10^8$, s^{-1}	K_{21}/K_{12}	$\sigma_{tr}/10^{-20}$, cm^2	$\lambda_{tr}/10^8$, s^{-1}	$\sigma_{tr}/10^{-20}$, cm^2	$\lambda_{tr}/10^8$, s^{-1}
0.001	FH-type Eqs.:	15.4	2.6	0.99	315.0	65.1	663.4	146.0
	[36]	15.8	2.7		384.4	80.0	828.7	170.0
	[37]	21.5	3.5		265.0	55.0	650.0	140.0
	[38]	18.0	2.8					
	[39]	14.2						
	Experiments:		2.8±0.5[58]			58.6±10[55]		84±13[54]
			2.8±0.3[57]					143±13[53]
			2.9±0.4[56]					95±34[52]
0.01	FH-type Eqs.:	4.84	2.6	0.99	99.1	64.7	208.1	144.8
	[36]	5.64			128.0		283.7	
	[37]	4.8			60.0		140.0	
	[38]	5.0						
	[39]	4.44						
0.04	FH-type Eqs.:	2.37	2.5	0.99	49.1	64.2	103.1	143.4
	[36]	2.94			63.6		140.7	
	[37]	3.1			40.0		91.0	
	[38]	2.5						
0.1	FH-type Eqs.:	1.42	2.4	0.99	30.7	63.5	64.6	142.1
	[36]	2.0			39.9		87.4	
	[39]	1.35						

TABLE II. The total cross sections $\sigma_{\overline{\mathrm{H}}}$ and $\sigma_{\overline{\mathrm{H}}_\mu}$ for the reactions (1) and (2) respectively. The product of these cross sections and the corresponding center-of-mass velocities $v_{c.m.}$ between $\overline{\mathrm{p}}$ and Ps=(e^+e^-), i.e. $\sigma_{\overline{\mathrm{H}}}v_{c.m.}$ and between $\overline{\mathrm{p}}$ and the true muonium atom $\mathrm{Ps}_\mu = (\mu^+\mu^-)$, i.e. $\sigma_{\overline{\mathrm{H}}_\mu}v_{c.m.}$ are presented.

	$\overline{\mathrm{p}} + (e^+e^-)_{1s} \to \overline{\mathrm{H}} + e^-$		$\overline{\mathrm{p}} + (\mu^+\mu^-)_{1s} \to \overline{\mathrm{H}}_\mu + \mu^-$	
E, eV	$\sigma_{\overline{\mathrm{H}}}$, cm^2	$\sigma_{\overline{\mathrm{H}}}v_{c.m.}$, cm^3/s	$\sigma_{\overline{\mathrm{H}}_\mu}$, cm^2	$\sigma_{\overline{\mathrm{H}}_\mu}v_{c.m.}$, cm^3/s
1.0e-06	0.16e-12	0.67e-08		
1.0e-05	0.50e-13	0.67e-08		
1.0e-04	0.16e-13	0.67e-08	0.18e-16	0.60e-12
1.0e-03	0.50e-14	0.66e-08	0.58e-17	0.60e-12
1.0e-02	0.15e-14	0.63e-08	0.18e-17	0.59e-12
5.0e-02	0.60e-15	0.56e-08	0.82e-18	0.59e-12
1.0e-01	0.42e-15	0.55e-08	0.58e-18	0.59e-12
5.0e-01			0.27e-18	0.62e-12
1.0e-00			0.23e-18	0.73e-12

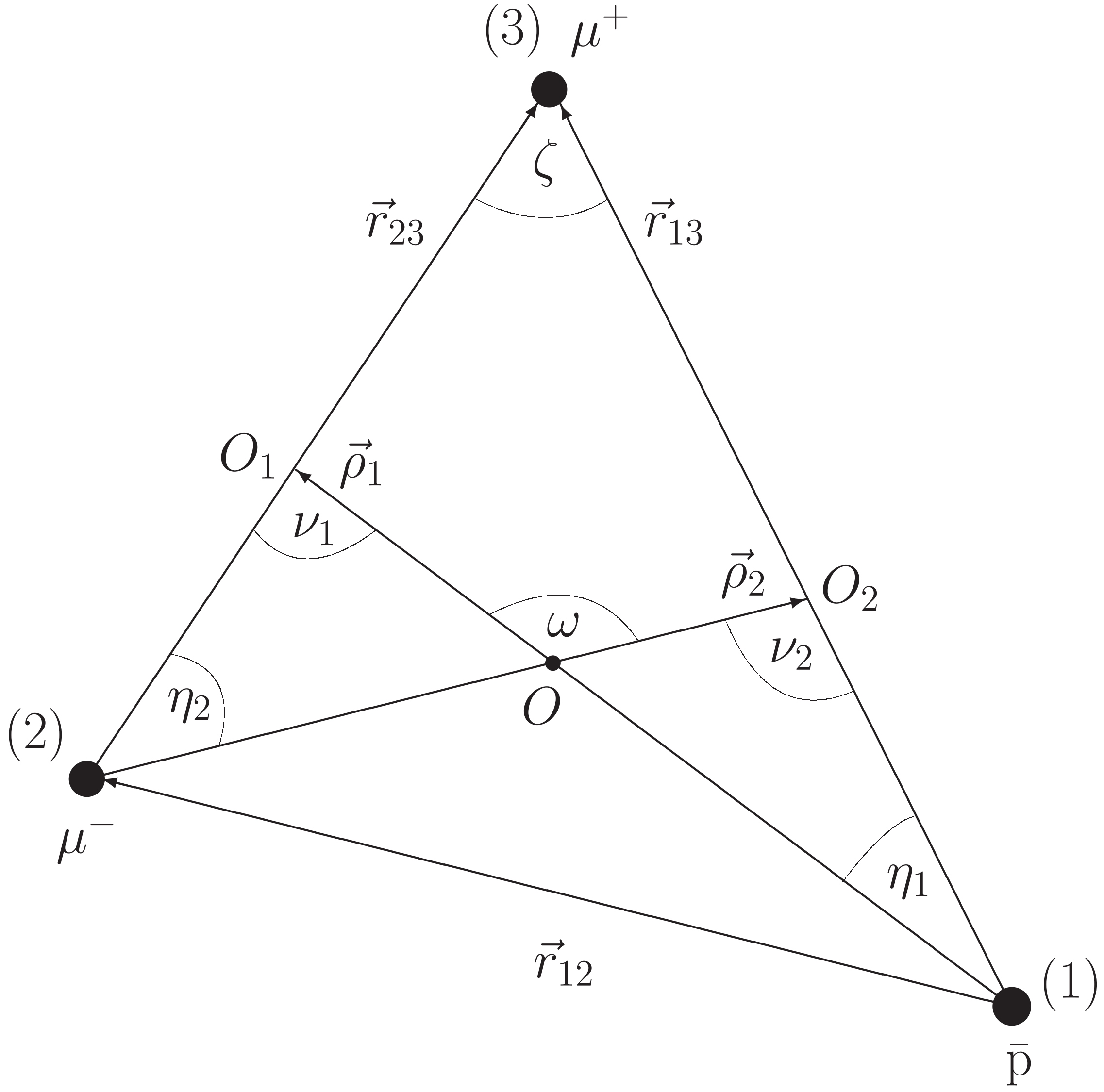

FIG. 1. The configurational triangle of a three-charged-particle system (123). ($\overline{\mathrm{p}}\,\mu^-\mu^+$) is presented together with the Jacobi coordinates, the inter-particle vectors, and the angles between the vectors and coordinates. O is the center of mass of the few-body system system, O_1 and O_2 are the center of masses of the targets $\mu^-\mu^+$ and $\overline{\mathrm{p}}\mu^+$ respectively.

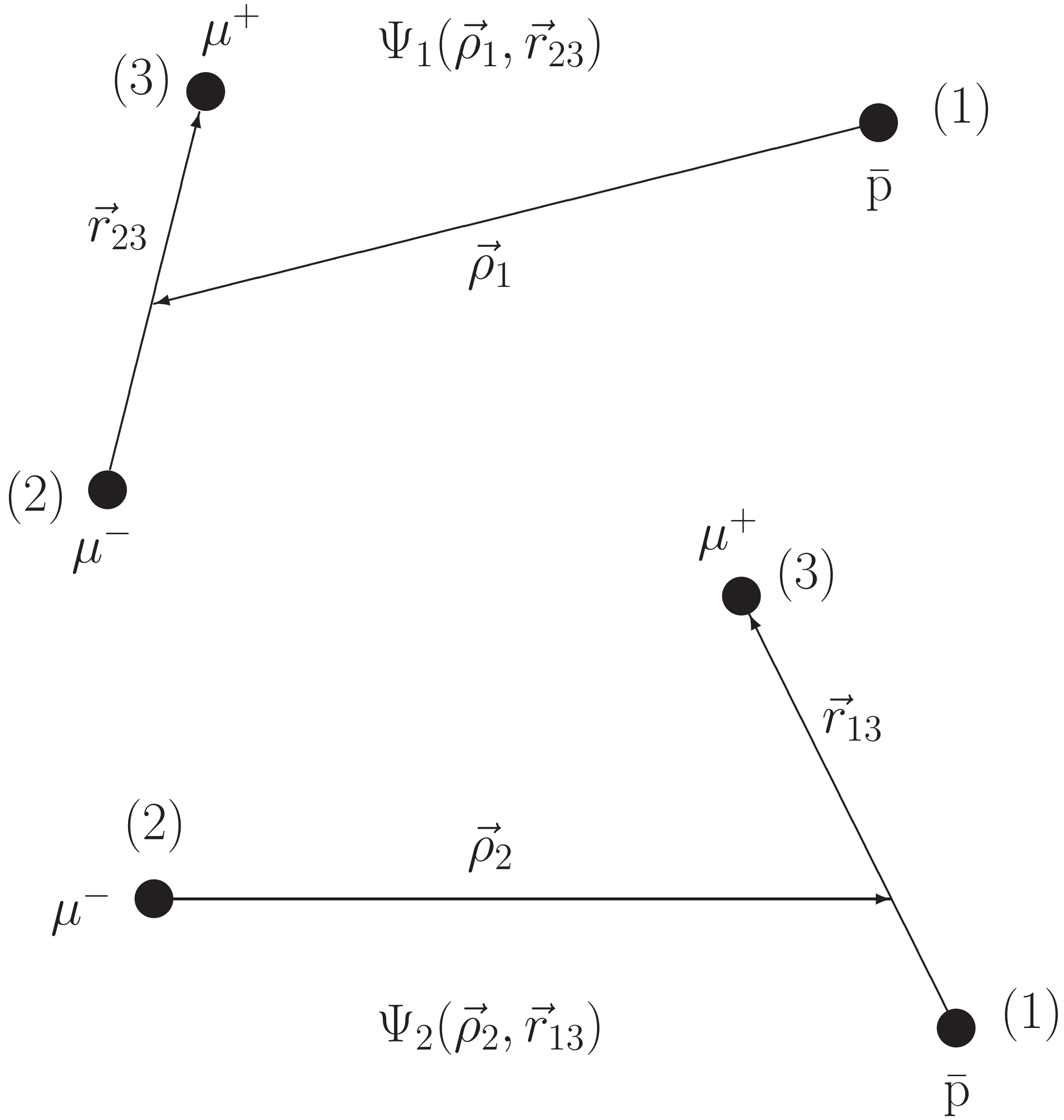

FIG. 2. Two asymptotic spacial configurations of the 3-body system (123), or more specifically $(\bar{\mathrm{p}}, \mu^-, \mu^+)$ which is considered in this work. The few-body Jacobi coordinates $(\vec{\rho}_i, \vec{r}_{jk})$, where $i \neq j \neq k = 1, 2, 3$ are also shown together with the 3-body wave function components Ψ_1 and Ψ_2: $\Psi = \Psi_1 + \Psi_2$ is the total wave function of the 3-body system.

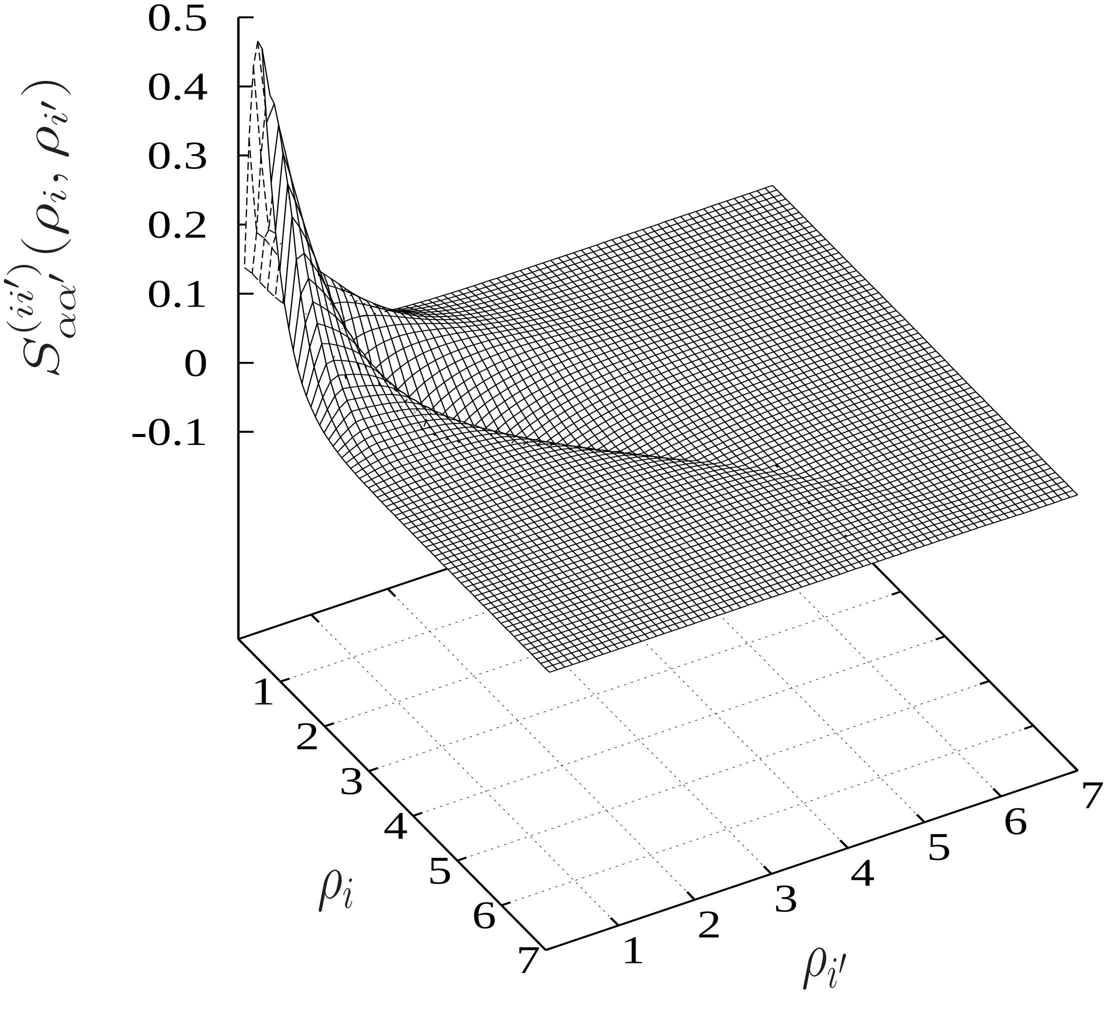

FIG. 3. The angular integral $S^{ii'}_{\alpha\alpha'}(\rho_i, \rho_{i'})$, Eq. (40), in the input channel $\overline{\mathrm{p}} + (\mu^+\mu^-)$ when α =1s and α' =1s.

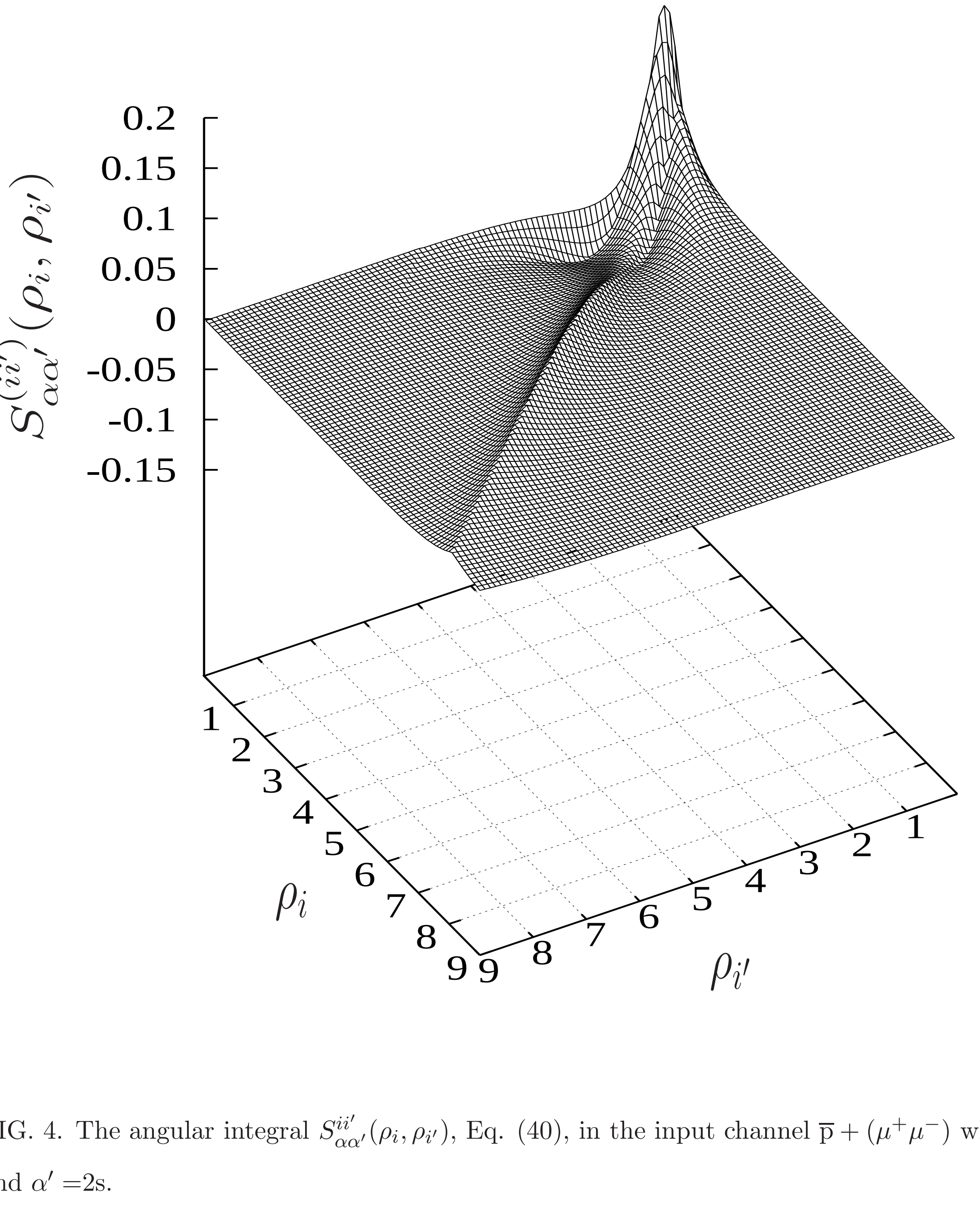

FIG. 4. The angular integral $S_{\alpha\alpha'}^{ii'}(\rho_i, \rho_{i'})$, Eq. (40), in the input channel $\overline{\mathrm{p}} + (\mu^+\mu^-)$ when α =1s and α' =2s.

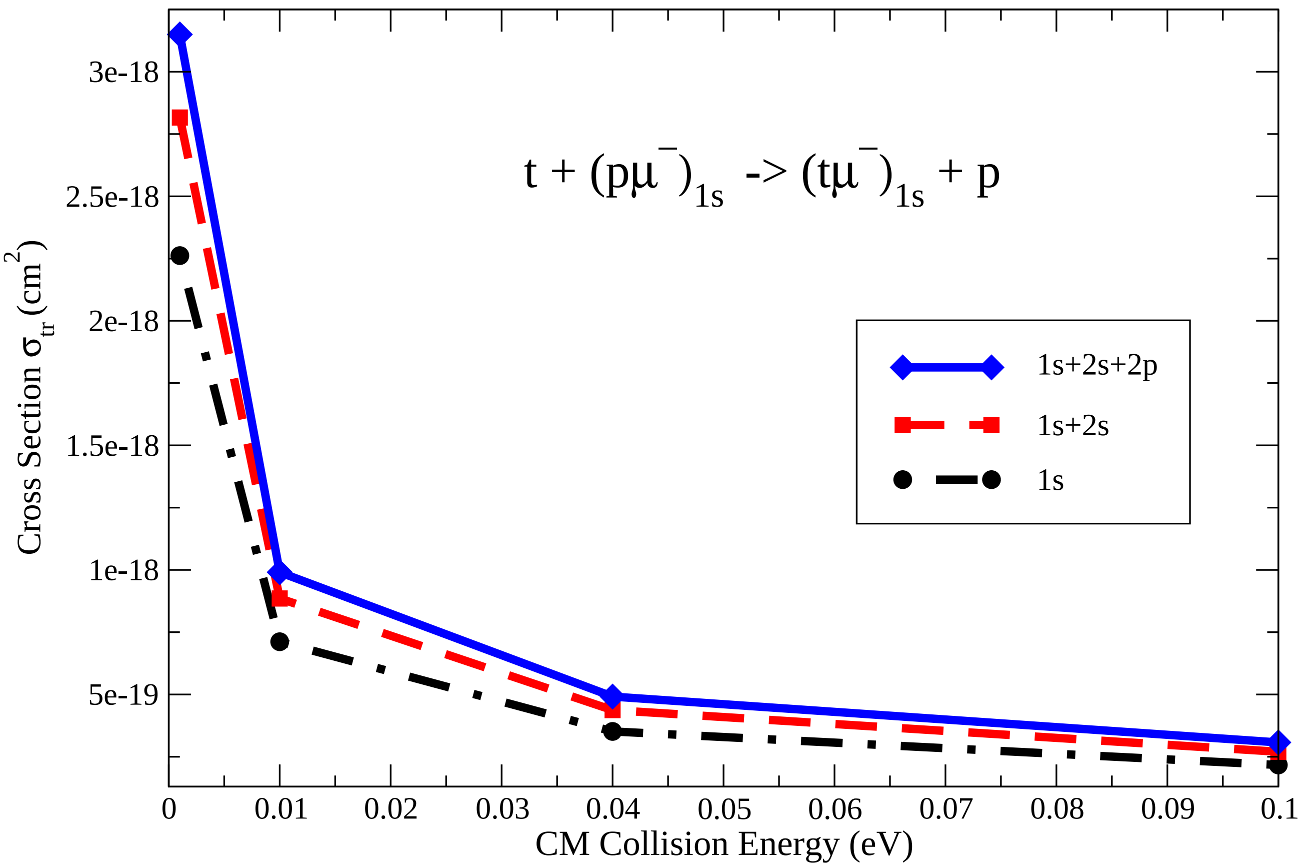

FIG. 5. Low energy cross sections for a muon transfer reaction in the t+$(p\mu^-)_{1s}$ collision. Results are shown for the two-level 2×1s, four-level 2×(1s+2s), and six-level 2×(1s+2s+2p) close-coupling approximations.

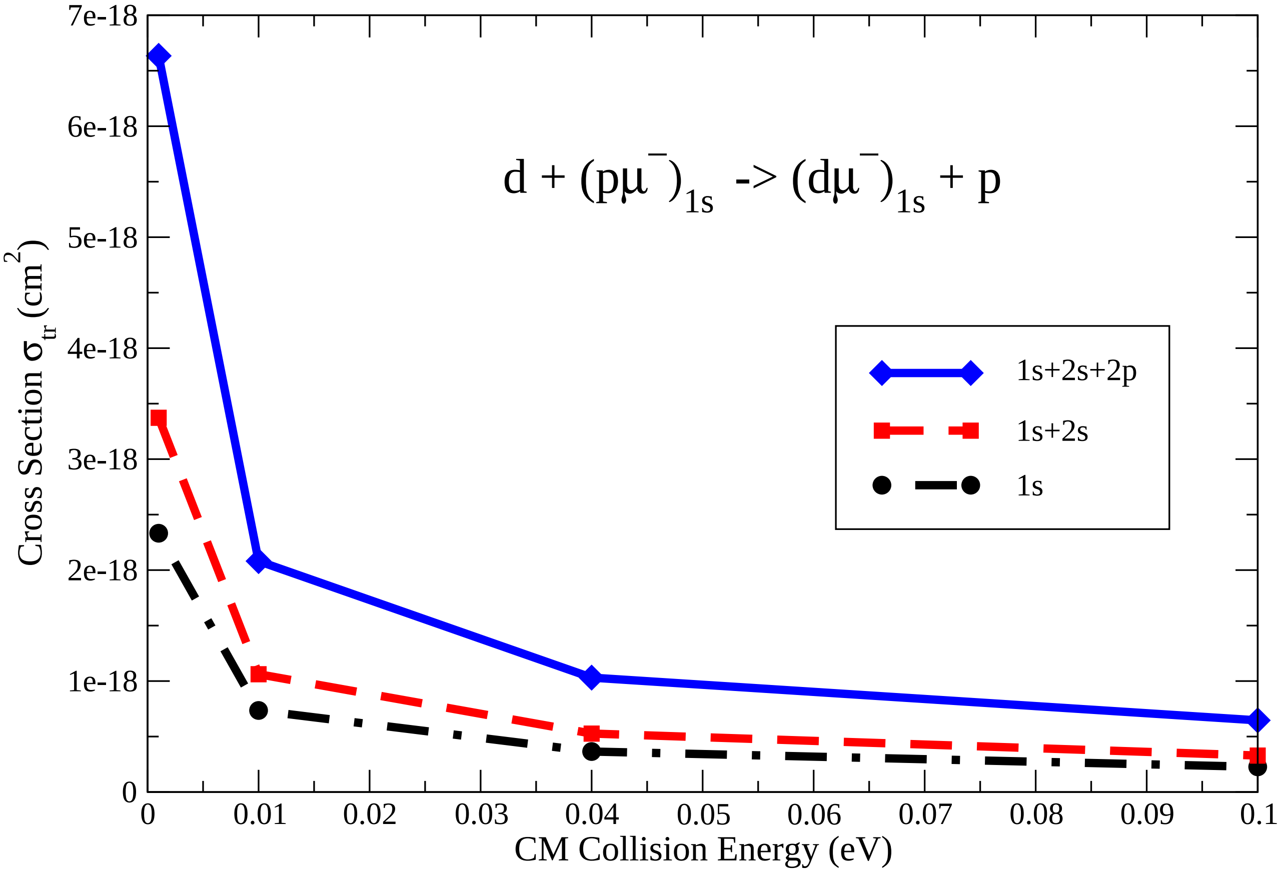

FIG. 6. Low energy cross sections for a muon transfer reaction in the d+$(p\mu^-)_{1s}$ collision. Results are shown for the two-level 2×1s, four-level 2×(1s+2s), and six-level 2×(1s+2s+2p) close-coupling approximations.

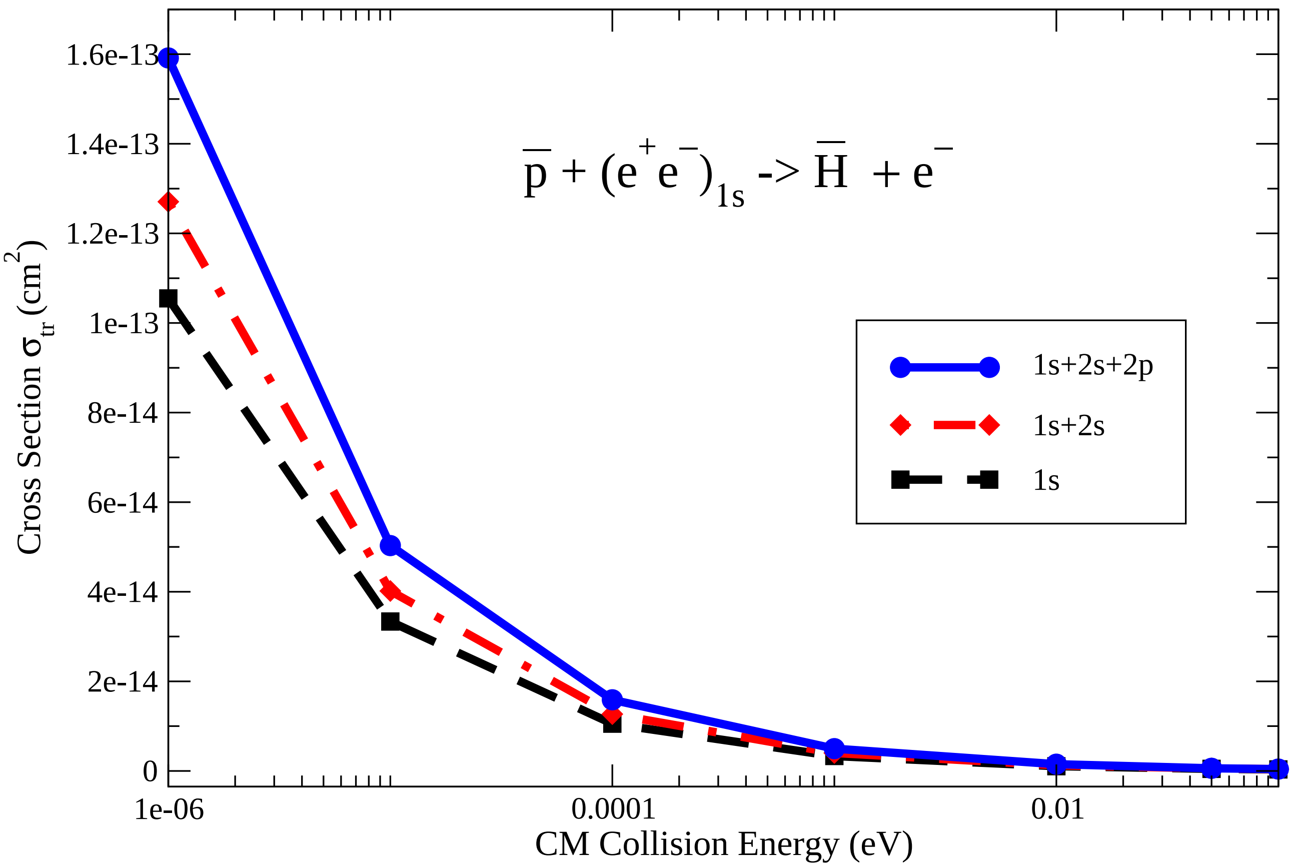

FIG. 7. Low energy cross sections for an antihydrogen atom formation reaction (1). Results are shown for the two-level 2×1s, four-level 2×(1s+2s), and six-level 2×(1s+2s+2p) close-coupling approximations.

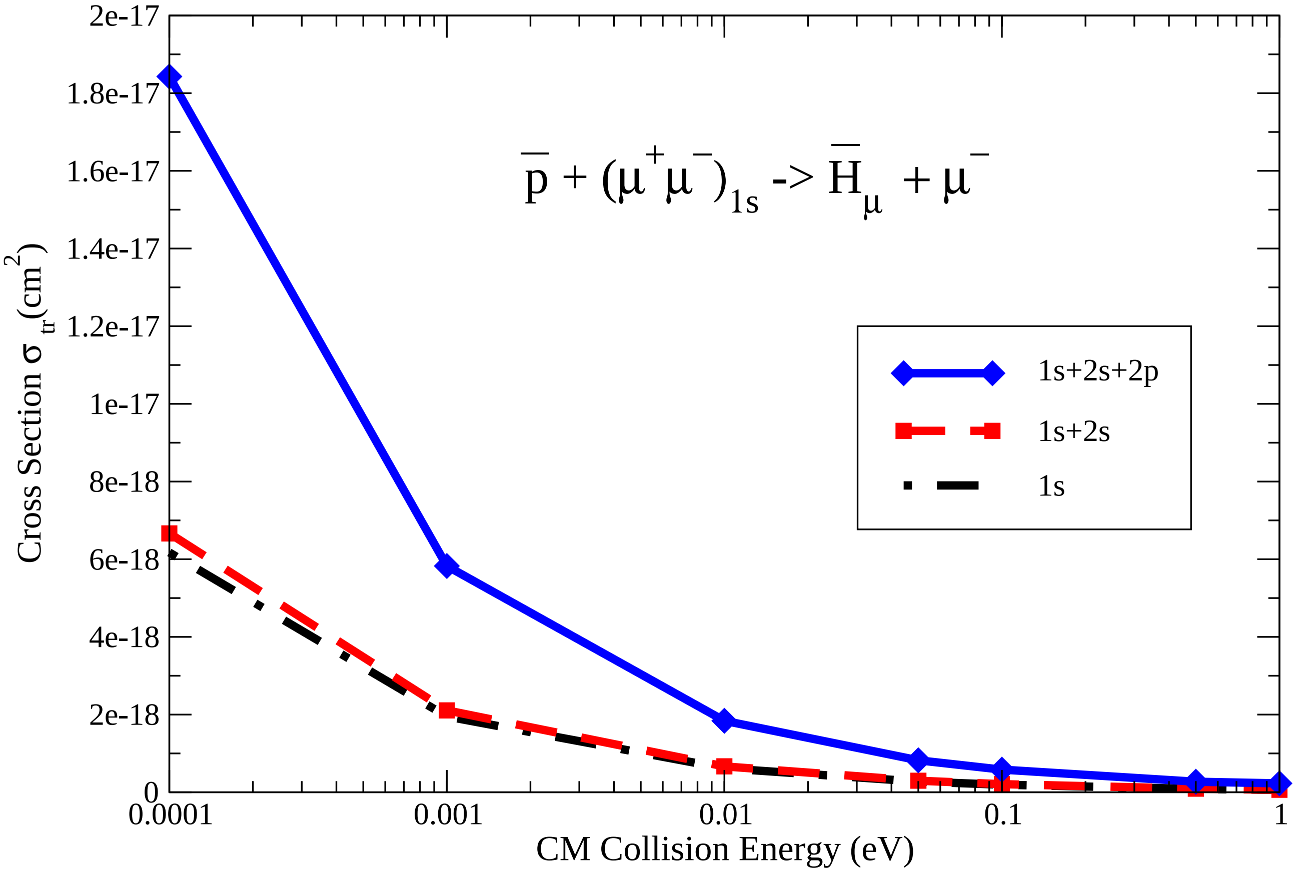

FIG. 8. Low energy cross sections for a muonic antihydrogen formation reaction (2). Results are shown for the two-level 2×1s, four-level 2×(1s+2s), and six-level 2×(1s+2s+2p) close-coupling approximations.

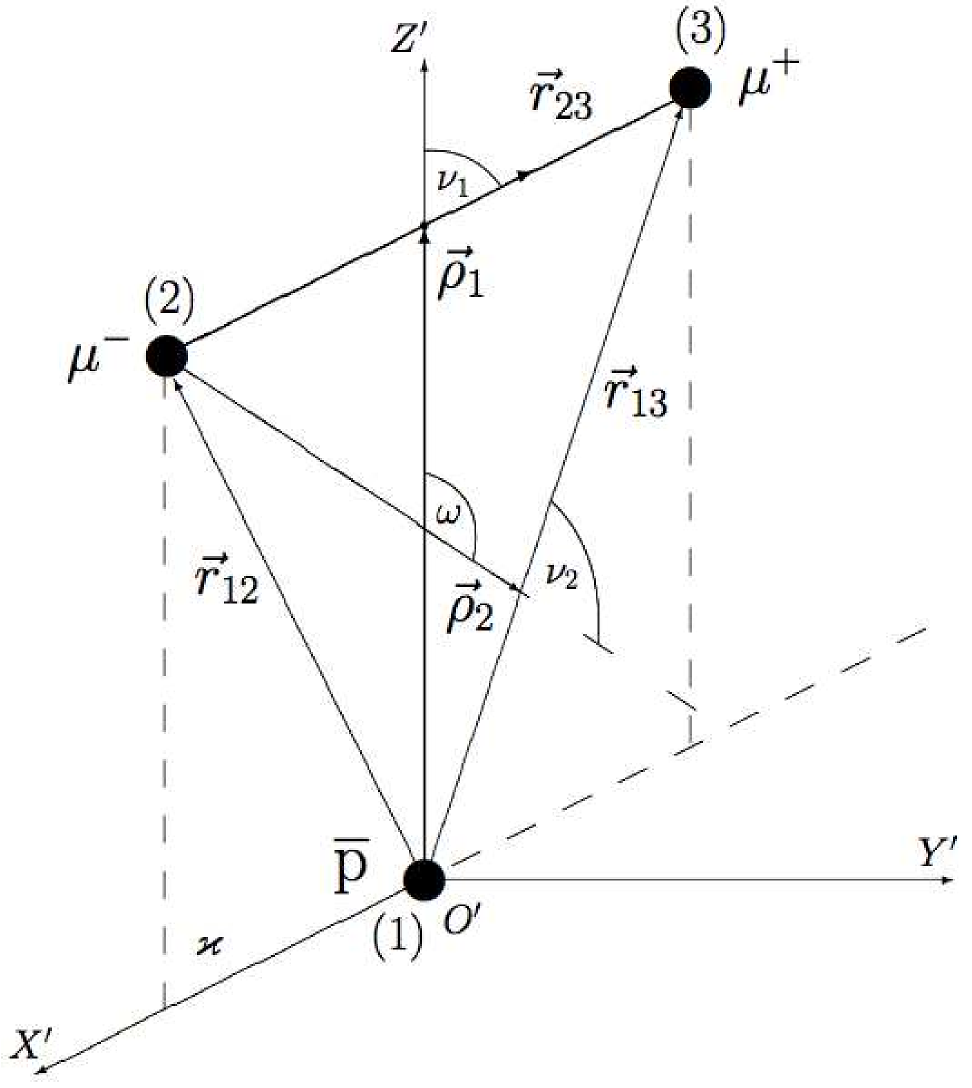

FIG. 9. The configurational $\triangle(123)$ in the case of the $\overline{\mathrm{p}}+(\mu^-\mu^+)$ collision is shown together with the new $O'X'Y'Z'$ cartesian coordinate system after the rotational-translational transformation from the initial $OXYZ$ system (see Appendix, Sect. IV). $OXYZ$ is not shown here.